TECHNICAL OPERATIONS RESEARCH

THE EFFECT OF INTERIOR PARTITIONS ON THE DOSE RATE IN A MULTISTORY WINDOWLESS BUILDING

By

Albert W. Starbird, Joseph D. Velletri
Robert L. MacNeil, and John F. Batter

Report No. TO-B 63-6
Contract No. OCD-OS-62-14
31 January 1963

Submitted to

Office of Civil Defense
Department of Defense
Washington, D.C.

techops

tech ops

TECHNICAL OPERATIONS RESEARCH

THE EFFECT OF INTERIOR PARTITIONS ON THE DOSE RATE IN A MULTISTORY WINDOWLESS BUILDING

By

Albert W. Starbird, Joseph D. Velletri
Robert L. MacNeil, and John F. Batter

Report No. TO-B 63-6
Contract No. OCD-OS-62-14
31 January 1963

Submitted to

Office of Civil Defense
Department of Defense
Washington, D. C.

Burlington, Massachusetts

ACKNOWLEDGMENTS

The authors are indebted to Mrs. Nancy-Ruth York, Mr. Milton Dwonczyk, and Mr. William Barch for their untiring efforts in the performance of the experiments described in this report.

ABSTRACT

This report evaluates the effects of three common types of interior partitions within multistory structures on the dose rates from infinite uniform fields of fallout contamination. Comparisons are made between experimentally determined steel model results utilizing cobalt-60 gamma radiation and those obtained through use of the OCD engineering manual entitled "Design and Review of Structures from Fallout Gamma Radiation." A comparison is also made between partition results from limited fields of contamination and previous experimentally determined limited-field results for similar structures without partitions.

Agreement is excellent between experimentally measured and computed infinite-field dose rates for the three partition geometries compared — typical box, corridor, and compartment types.

TABLE OF CONTENTS

LIST OF ILLUSTRATIONS

LIST OF TABLES

CHAPTER 1

INTRODUCTION

The above-ground floors within multistory urban structures may provide an important potential shelter space from fallout radiation in the event of a nuclear attack on the United States. The shielding effects of many building components have to be considered in estimating the protection offered by these structures. The purpose of this study is to evaluate the present procedures for estimating the shielding influence of one of these components -- the interior partitions in a multistory building.

The program objective has been to evaluate the procedures used in the manual entitled "Design and Review of Structures for Protection from Fallout Gamma Radiation"[1] to account for the shielding effects of interior partitions. Experimental data on the effects of interior partitions in real geometries were required to accomplish this. These data were obtained through a series of measurements made on a steel scale model of a 6-story structure 36 x 48 x 72 feet high. The basic model was the same as that previously used in a study of the effects of limited strips of contamination on a multistory building. For the current study three typical interior partition geometries were added to the structure: (1) a box-type central core room, (2) a 6-foot-wide corridor running lengthwise through the building, and (3) a corridor plus dividing right-angle partitions that formed four equal-sized compartments on each side of the corridor. Three mass thicknesses of each partition geometry were tested for their effects on dose rates within the structure.

Chapter 2 contains a complete description of the experimental procedures, the structure geometries investigated, and the data obtained. Analytical analysis and the comparisons of experimental and calculated results are given in Chapter 3. Chapter 3 also gives a comparison between experimental finite field results of this study with those obtained in previous studies on the effects of limited strips of contamination[2,3] for a similar structure without partitions. Conclusions and recommendations gained from this study are contained in Chapter 4.

CHAPTER 2

DESCRIPTION OF EXPERIMENT

THE MODELING TECHNIQUE

Theoretically the radiation-dose distribution inside a structure from radiation sources located outside a structure will be exactly reproduced in a geometrically similar scale model if the densities of all materials comprising the structure, the surrounding ground, and the atmosphere are increased by a scale factor. Perfect scaling would therefore require that: (1) all physical dimensions be linearly scaled by the same factor, (2) each absorbing surface attenuate radiation to the same degree as the original surface, independent of the scaling factor, and (3) the specific scattering and absorption properties of all materials remain unchanged. These basic rules of modeling show that densities of all materials should be increased by the same scaling factor that reduces linear dimensions.

In practice, however, the problem of increasing densities by a factor large enough to be useful in reducing building dimensions makes it difficult to achieve this ideal. For modeling to have sufficient advantage over full-size structure experimentation, scaling by a factor of at least 10 must be used. A scale factor of 12 was employed for the 6-story model building used in the experiment covered in this report. The actual scaling rules followed in this experiment were somewhat relaxed from those defining perfect modeling. Iron was substituted for concrete and other building materials to increase density without radically changing the atomic number and the corresponding cross sections of the material. This permitted an increase in average density of approximately 3 as compared to the desired factor of 12. However, prior modeling experiments[4,5] have shown that realistic results can be obtained if the wall thickness does not exceed 10% of the average dimensions of any given room. Hence, wall thicknesses may be increased above those indicated by the scale factor without seriously distorting the dose distribution within the structure.

Since it is impractical to scale the densities of the ground or atmosphere surrounding the models, skyshine and ground penetrations were not properly reproduced in the experiment and must be allowed for by analytical procedures. However, since skyshine comprises a maximum of 10% of the dose rate for a zero thickness building and attenuates more rapidly than direct or structure-scattered radiation, the error

due to neglect of skyshine should be small. The model building is thick enough so that most of the radiation within the structure is direct radiation from the gamma-ray source or from radiation scattered by the walls and ceilings of the building itself.

SCALE MODEL STRUCTURE

EXPERIMENTAL BUILDING

Shielding experiments were conducted on a 6-story, steel model structure scaled 1/12 full-size, representing a building 72 feet high with a rectangular plan area 36 x 48 feet. Each story of the model was 12 inches high. The structure had no doors or windows, and all walls, floors, and ceilings were composed of one or more plates of hot rolled steel. The walls of the model for this series of experiments contained one thickness (20 psf) of 1/2-inch plate. The floors of the model contained four thicknesses (80 psf) of 1/2-inch plate; the 2-inch (80 psf) floors reduced the open distance between floor and ceiling to 10 inches.

Results on experiments previously conducted[2,3] on this basic building without interior partitions are included in this report for comparison. The structure designs evaluated in this study are identical with the basic building used in earlier experiments except that three different types of partition arrangements are interposed. The three arrangements and mass thickness variations used for the model tests are as follows:

1. Box Partitions (Figure 1a)—A rectangular room, located at the center of a building story, with walls parallel to the exterior walls. Model tested with partition mass thicknesses of 20, 40, and 60 psf.
2. Corridor Partitions (Figure 1b)—A 6-inch-wide corridor running lengthwise through the model building. Mass thicknesses tested were 20, 40, and 60 psf.
3. Compartmental Partitions (Figure 1c)—Four equal-sized compartments on each side of a 40 psf corridor 6 inches wide. Compartment partitions were perpendicular to the corridor and were tested at 10, 20, and 40 psf thicknesses.

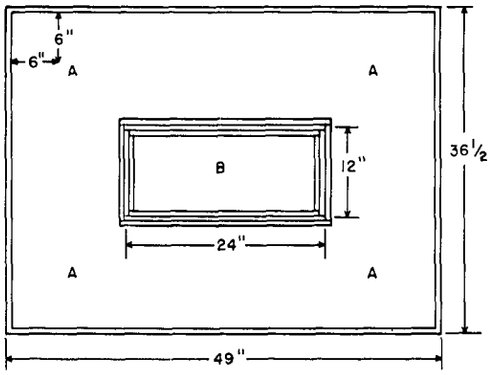

a. Box Geometry, 60 psf Partitions

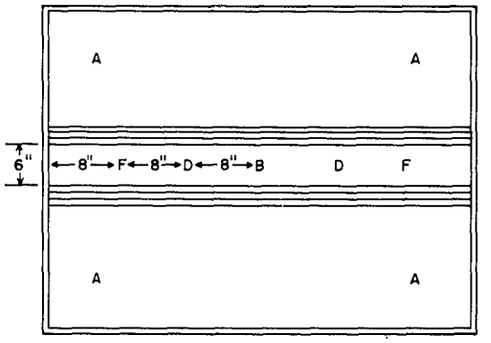

b. Corridor Geometry, 60 psf Partitions

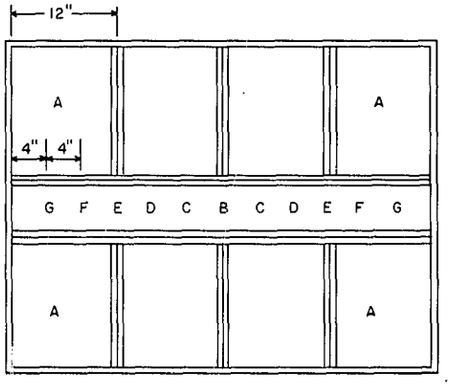

c. Compartment Geometry, 40 psf Partitions

Figure 1. Partition Arrangements

The 10 psf partitions were assembled from 1/4-inch thick steel plate, while 20, 40, and 60 psf walls were comprised of 1, 2, and 3 thicknesses of 1/2-inch steel plate respectively. Access to dosimeters within the structure was gained by removing the rear or side wall and the appropriate box partition. Figure 2 illustrates the model structure with 60 psf box-type partitions and shows the back wall of the box removed for dosimeter access.

All partition arrangements contained quarter symmetry, thus reducing to one quadrant the required simulated area of contamination for these experiments.

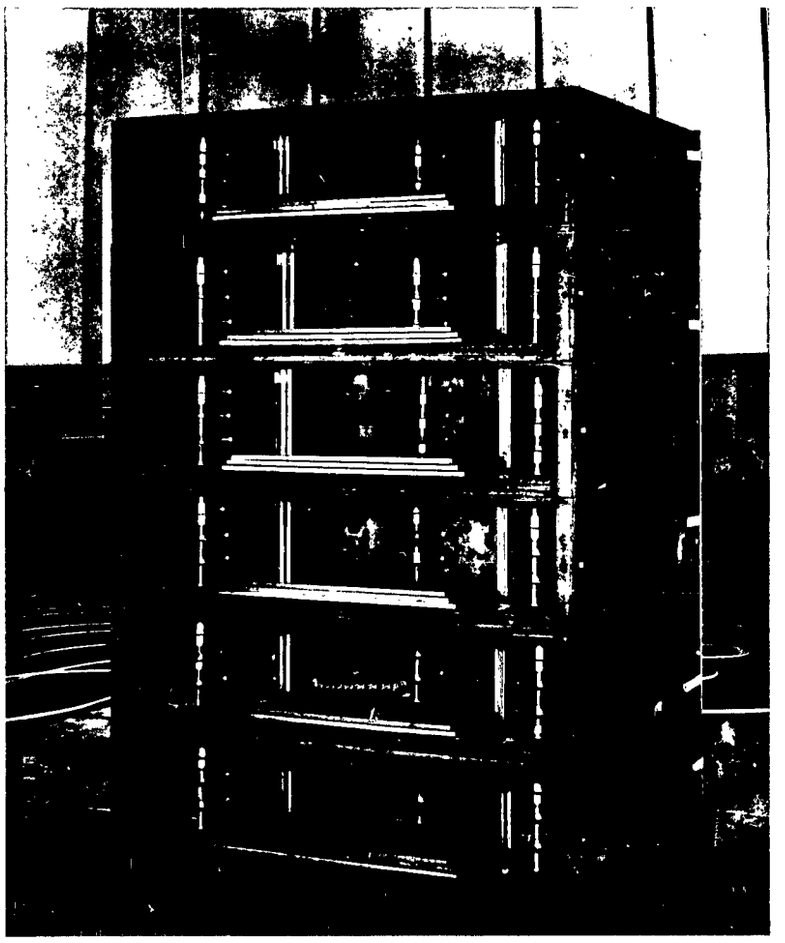

Figure 2. Multistory Structure with Box-Type Partitions (Rear panel removed and boxes open for access to dosimeters)

SIMULATION OF CONTAMINATED AREAS

The source area quadrant was broken into eight individual segments, as shown in Figure 3. The first five of these segments represented quarter rectangular annuli.

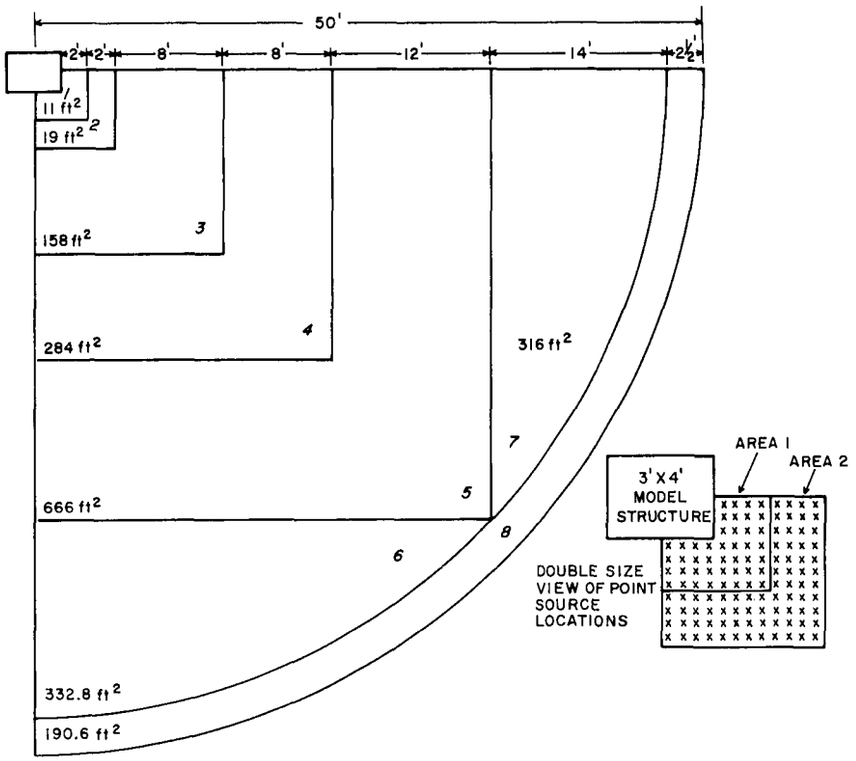

Figure 3. Areas of Simulated Fallout Contamination

Areas 6 and 7 completed a circular quadrant 47.7 feet in radius, while Area 8 provided a quarter annulus 2-1/2-feet wide to give data useful in the analytical estimate of far-field effects. Areas of contamination were simulated by appropriate orientation of cobalt-60 sources over each area. Contamination in areas close to the model was simulated through placement of point sources at evenly spaced inter-

vals, while simulation of contaminated areas located 4 feet or more from the model was created by pumping a source at constant velocity through prepositioned tubing over an entire area. Figure 4 shows a partial view of these areas.

Tubing and point sources were positioned so that the dose accumulated by integrating-type detectors within the model would be equivalent to that received if the source were uniformly smeared over the source area.

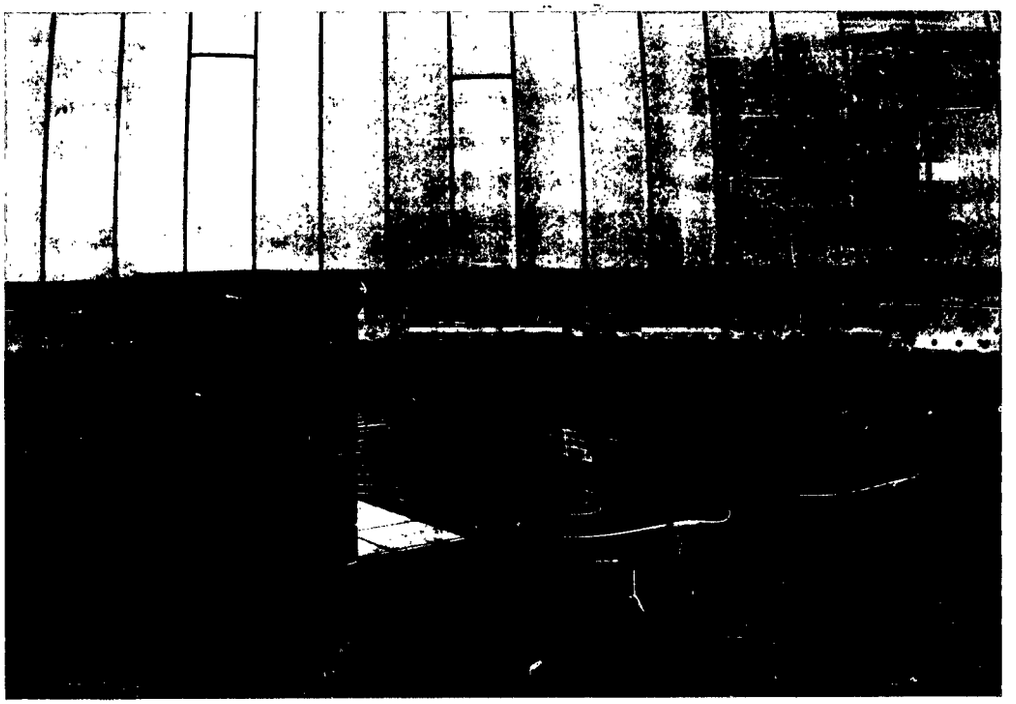

Figure 4. View of Simulated Fallout Quadrant

POINT SOURCES

Rod-mounted sources were manually placed on Areas 1 and 2 to simulate contaminated areas. A 0.50-curie cobalt-60 source was used for the point-source work. Point-source locations were marked at 6-inch intervals, starting at 3 inches from

the outer wall of the model. Area 1, which was 11 square feet, had 44 points, and Area 2, 19 square feet, had 76 points. The source was placed in each position an equal length of time. The source handling rod was 14 feet long, limiting dose rates to the operator to about 35 mr/hr.

PUMPED SOURCE

A uniform density of contamination was simulated in Areas 3 through 8 by pumping a cobalt-60 source of approximately 23 curies strength through properly arranged polyethylene tubing. The tubing was spaced so that the source traveling at a uniform velocity through the tubing would spend an equal amount of time in each square foot of the area being simulated. The detectors in the model integrate the effects of radiation from each increment of tubing as the source passes through it, thus presenting in effect an essentially uniform source area density. The polyethylene tubing used had an internal diameter of 0.267 inch with a 1/8-inch wall thickness.

In Areas 3, 4, 5, 6, and 7 the tubing was placed at 1-foot intervals. Each loop ran the entire length of the quarter annulus with 1-foot radius turns at the ends. Tubing in Areas 6 and 7 also was placed with 1-foot spacing, while Area 8 contained three loops of tubing running the full length of the quarter annulus spaced at 10-inch intervals. The tubing leads from the source container were shielded with lead shot to a minimum thickness of 6 inches to prevent the presence of source motion within the leads from contributing detectable dosage values at the model building.

The equipment required for pumping an encapsulated source through the polyethylene tubing is similar to that previously developed and used by Technical Operations, Inc., for model and full-scale building tests. This type of equipment was described in detail in previous reports[6,7,8] and will therefore not be covered in detail in this report.

A schematic of the hydraulic system for source circulation is shown in Figure 5. Water from the reservoir is drawn into the appropriate pump or pumps and then forced through the source container. This operation drives the source out of the container, through the polyethylene tubing, and back to the storage container at the conclusion of the exposure. Flow from the pumps passes into a 3-way solenoid valve wired for remote operation. This valve allows either bypassing the pump

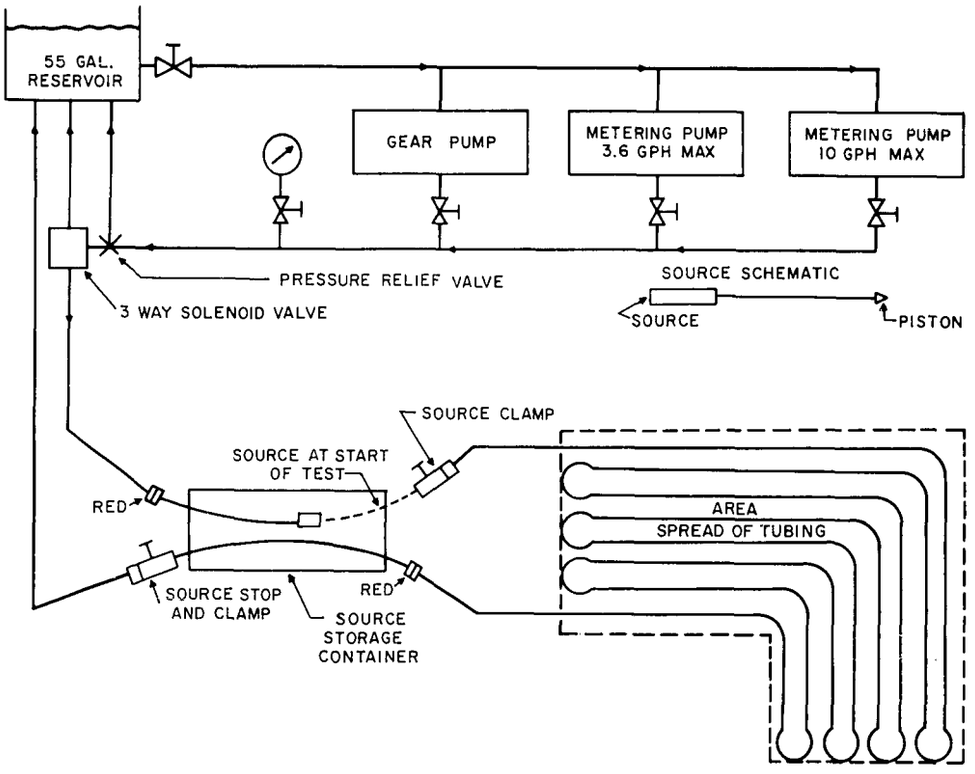

Figure 5. Diagram of Source Circulation System

output directly to the reservoir or diverting the flow to the source storage container and hence into the area spread of tubing. The source container is a 1000 pound lead-filled steel shell mounted on wheels. Two stainless-steel tubes of the same internal dimensions as the polyethylene tubes pass lengthwise through the center of the container.

INSTRUMENTATION

Measurements in the model building were generally made with Victoreen Model 362 (200 mr) pocket dosimeters; in areas of exceptionally low accumulated dose, Victoreen Model 239 (10 mr) stray radiation chambers were used. The charger-

reader instruments used in conjunction with the dosimeters were portable units specifically designed and constructed by Technical Operations, Inc., for field experiments. These units, which have been described in detail previously,[9] operate on the principle of measuring the electrical charge required to return a dosimeter to the voltage to which it was charged before an exposure.

Since dosimeter length is large (5-1/2 inches) in relation to the floor heights, the dosimeters were always mounted horizontally and parallel to the source area to ensure that a minimum dose-rate gradient existed over the dosimeter length. The detectors were placed 2-1/2, 5, and 7-1/2 inches above each floor for the box and corridor geometries. The compartment configuration was, however, instrumented only on the first, third, and fifth floors. Dosimeter stands were constructed of phenolic tubing 3/4 inch in diameter by 1/32 inch thick to minimize their effect on the readings. These stands were then mounted on a 1/32-inch Bakelite base fitted into a second base that was glued to the structure to allow accurate reproducible placement of the dosimeters. Calibration checks with and without these stands showed that there was no measurable gamma-ray attenuation or backscattering from the stands.

The detectors for the box partition geometry were placed to form five vertical building traverses, one at each corner plus a center traverse. The corner positions were located 6 inches perpendicular from the walls, and the center position was located in the center of the box partitions (see Figure 1a). In the corridor geometry, vertical traverses were also formed at 8-inch intervals along the corridor (see Figure 2); in the compartment geometry ten vertical traverses were formed in the corridors on the first, third, and fifth floors at 4 inch intervals along the corridor, in addition to those located at the center and the corners of the structures.

CALIBRATION

For this experiment, the instruments used in conjunction with the Tech/Ops charger-reader were 10 mr and 200 mr full-range ionization detectors. Since the output of these charger-readers is presented upon an arbitrary scale ranging from 0 to 100, they were calibrated by exposing the chambers to a cobalt-60 source previously calibrated by the National Bureau of Standards. This calibration was performed on an essentially mass-less calibration range with source-to-detector dis-

tance equal to 1/4 of the source and detector-to-ground distance, thus giving expected total dosage within 1% of free-air values.[10] Recalibration was performed periodically to detect variations in instrument performance.

EXPERIMENTAL DATA

Experiments on the model structure were conducted at the Radiation Model Facility at Technical Operations Research, Burlington, Massachusetts. The model structure, erected at the center of a 50-foot radius asphalt surface, was subjected to gamma radiation exposures from eight individual areas (Figure 3) of simulated fallout contamination that together comprised a circular quadrant 50.2 feet in radius. Dose measurements were made at the four corner positions and the center position for all three experimental configurations. Measurements were also made within the corridor at four off-center positions for the corridor experiment, and ten off-center positions for the compartment experiment. All dosimeter readings obtained from these experiments were corrected for temperature and pressure and normalized to a roentgen per hour basis from an equivalent source density of 1 curie per square foot.*

The raw data from each of the source fields were then multiplied by an appropriate factor to account for the effects of the anisotropy of the cobalt-60 source and the gamma-ray attenuation from the inner lengths of the source tubing when the source is in the extreme radial position in each source area. This factor was obtained by dividing the dose rates obtained from a vertical traverse at the center of a zero mass thickness version (phantom building) of the multistory model exposed to the actual experimental field by dose rates previously obtained from a distribution of point isotopic sources. The phantom building data are given in Table 1, and the correction factors for source anisotropy and tubing attenuation for each source field are presented in Table 2. The method of determining these correction factors from the phantom building data is covered in detail in Chapter 3 of Reference 3.

The normalized dose rate levels for the compartmentalized multistory structures after application of the source anisotropy and tubing correction factors are

*This source density creates a field of 497 r/hr at a 3-foot height above an infinite, smooth, uniformly contaminated plane. (Reference 5.)

TABLE 1

DOSE RATE VS HEIGHT FOR PHANTOM STRUCTURE
(Normalized to 1 curie/ft^2 cobalt-60)
(r/hr)

Area	Detector Height (Inches)													
	3	6	9	12	18	24	30	36	42	48	54	60	66	72
1	15.14	15.17	14.80	13.99	12.48	10.68	9.18	7.76	6.55	5.51	4.65	3.95	3.58	3.05
2	8.64	9.46	9.40	9.12	8.88	8.28	7.80	7.10	6.50	5.84	5.32	5.03	4.63	3.98
3	16.80	17.16	16.68	17.64	17.04	16.80	17.04	16.44	16.32	16.30	15.12	14.64	14.28	13.44
4	8.19	8.58	8.51	8.98	8.90	8.90	9.06	8.82	9.29	9.06	8.82	8.82	8.90	8.35
5	7.71	8.26	8.53	8.81	8.67	8.67	8.81	8.67	9.08	8.94	9.08	8.94	9.08	8.81
6	1.68	1.69	1.83	2.08	1.92	1.96	2.68	2.08	2.12	2.12	2.20	2.20	2.20	2.20
7	1.06	1.48	1.62	1.69	1.76	1.79	1.90	1.90	1.90	1.94	1.94	1.97	2.01	1.97
8	0.39	0.59	0.74	0.87	0.87	0.94	0.97	1.04	1.00	1.00	1.03	1.00	1.03	1.00

TABLE 2

MULTIPLICATIVE CORRECTION FACTOR TO ALLOW FOR SOURCE ANISOTROPY AND TUBING ATTENUATION

Floor	Detector Height (Inches)	Experimental Areas (see Figure 3)				
		1	2	3-5	6-7	8
1	2.5	1.0	1.3	1.3	2.0	3.0
	5.0	1.0	1.2	1.3	1.7	2.0
	7.5	1.0	1.2	1.3	1.6	1.6
2	2.5	1.0	1.1	1.2	1.5	1.3
	5.0	1.0	1.1	1.2	1.5	1.3
	7.5	1.0	1.1	1.2	1.5	1.3
3	2.5	1.0	1.1	1.2	1.4	1.2
	5.0	1.0	1.1	1.2	1.4	1.2
	7.5	1.0	1.1	1.2	1.4	1.2
4	2.5	1.0	1.1	1.2	1.4	1.2
	5.0	1.0	1.1	1.2	1.4	1.2
	7.5	1.0	1.1	1.2	1.4	1.2
5	2.5	1.0	1.1	1.2	1.4	1.2
	5.0	1.0	1.1	1.2	1.4	1.2
	7.5	1.0	1.1	1.2	1.4	1.2
6	2.5	1.0	1.1	1.2	1.4	1.2
	5.0	1.0	1.1	1.2	1.4	1.2
	7.5	1.0	1.1	1.2	1.4	1.2

presented in Tables 3, 4, and 5. Each table presents the measured dose rate values from a 360-degree finite source field at specific locations within the model. Position A is at a building corner, B at the center, and C, D, E, F, and G at the off-center corridor positions. As the quarter symmetry technique (source fields covering only a quarter annulus) was used experimentally, raw data for center positions had to be multiplied by 4 to obtain the 360-degree finite field results presented in the tables. Off-center corridor data were converted to full annulus results by adding the reading of a C, D, E, F, or G detector to a symmetrically placed detector at the opposite side of the corridor and then multiplying the sum by 2. Results from the four corner positions of the model were summed to obtain full annulus values.

To illustrate the general trend of the variation of dose rate with detector position and interior partition mass thicknesses, several typical plots are presented in Figure 6. Figure 6a presents dose rate values for the corner position at the mid-floor height for the 0, 20, 40, and 60 psf box partitions. Comparison of these curves shows that the corner position is not significantly affected by increasing the mass thickness of the interior partitions.

Figure 6b presents dose rate values for the box-partition center position. These curves illustrate the effectiveness of increasing interior partition mass thickness on the dose measured at the center position.

Figure 6c illustrates the variation of dose rate in the corridor with location for three floor and three corridor wall mass thicknesses. Dose distribution in the corridor for the compartment experiment is shown in Figure 6d for the first, third, and fifth floors.

TABLE 3

DOSE RATE IN MODEL BUILDING, BOX PARTITION
(r/hr normalized to source density of 1 curie/ft^2)

Thickness Interior Partition (psf)	Area 1						Area 2						Area 3						Area 4					
	Floor 1						Floor 1						Floor 1						Floor 1					
	Position A			Position B			Position A			Position B			Position A			Position B			Position A			Position B		
	2-1/2"	5"	7-1/2"	2-1/2"	5"	7-1/2"	2-1/2"	5"	7-1/2"	2-1/2"	5"	7-1/2"	2-1/2"	5"	7-1/2"	2-1/2"	5"	7-1/2"	2-1/2"	5"	7-1/2"	2-1/2"	5"	7-1/2"
0	49	51	46	26	34	40	34	34	32	31	30	32	62	64	64	61	63	63	29	29	29	29	29	30
20	49	50	44	16	22	24	30	30	29	20	20	26	57	59	56	40	42	42	26	27	26	19	20	20
40	49	49	44	10	13	15	30	29	28	12	12	12	54	56	54	24	25	25	24	25	25	12	12	12
60	49	49	44	7.0	8.3	9.8	31	31	30	7.2	6.7	6.8	54	56	53	15	17	16	25	26	25	7.2	7.7	7.6
	Floor 2						Floor 2						Floor 2						Floor 2					
0	6.9	13	15	2.9	3.4	3.7	18	21	20	4.0	5.4	13	44	51	55	22	52	57	25	29	29	27	30	29
20	6.7	14	15	1.9	2.3	2.6	17	20	20	2.8	4.8	9.8	46	53	54	18	35	38	25	28	27	18	20	19
40	6.6	13	15	1.3	1.5	1.7	17	21	20	1.9	3.2	5.8	45	50	51	11	20	23	23	26	26	11	12	12
60	6.6	14	14	.85	.93	1.0	17	20	19	1.1	2.1	3.6	45	49	52	7.7	13	15	24	26	25	6.5	7.5	7.4
	Floor 3						Floor 3						Floor 3						Floor 3					
0	2.5	3.2	5.3	1.1	1.4	1.6	5.2	13	14	2.2	3.1	3.6	37	42	45	12	25	42	21	25	28	14	28	30
20	2.5	3.2	5.0	.69	.93	.97	5.2	13	14	1.4	1.9	2.3	37	43	46	9.2	17	27	22	24	26	10	18	19
40	2.5	3.1	4.8	.49	.61	.61	5.1	12	14	.98	1.2	1.5	35	40	42	4.7	11	16	23	24	25	6.4	11	12
60	2.7	3.3	5.2	.33	.40	.39	5.0	12	13	.45	.77	.90	36	41	43	3.4	7.6	11	21	24	25	4.2	7.0	7.2
	Floor 4						Floor 4						Floor 4						Floor 4					
0	1.3	1.4	1.7	.69	.75	.93	3.3	6.3	8.3	1.5	1.9	2.2	28	38	38	7.7	14	26	21	23	27	6.4	23	29
20	1.3	1.5	1.7	.23	.33	.37	2.6	6.4	8.4	.94	1.2	1.3	28	38	39	5.2	9.1	16	21	22	25	5.2	16	18
40	1.3	1.4	1.7	.14	.18	.21	2.9	6.4	9.2	.67	.77	.76	25	35	36	3.5	5.8	11	20	22	24	3.6	9.4	11
60	1.3	1.5	1.8	.081	.10	.12	2.9	6.3	9.0	.54	.33	.64	26	36	37	2.5	4.3	6.8	21	22	24	2.6	5.9	7.1
	Floor 5						Floor 5						Floor 5						Floor 5					
0	.79	.90	.95	.16	.28	.36	1.9	2.8	4.4	.85	1.1	1.3	17	30	33	6.6	7.9	13	20	21	23	4.4	14	25
20	.70	.79	.88	.085	.15	.16	2.0	2.9	4.7	.41	.62	.85	17	30	33	4.1	5.3	9.6	19	22	23	3.5	10	17
40	.64	.73	.81	.057	.069	.085	2.1	3.0	5.1	.29	.35	.45	16	29	30	2.7	3.6	6.1	19	21	22	2.8	6.1	9.5
60	.65	.73	.81	.033	.041	.045	2.0	2.9	5.0	.19	.21	.23	16	30	32	1.9	2.5	4.1	19	21	23	1.8	4.0	6.1
	Floor 6						Floor 6						Floor 6						Floor 6					
0	.40	.48	.57	.16	.18	.18	1.4	1.8	2.8	.54	.67	.80	12	24	28	4.3	5.7	8.5	18	20	21	4.2	8.6	21
20	.33	.40	.47	.061	.073	.089	1.4	1.8	2.8	.24	.33	.46	11	24	27	2.9	3.8	5.5	18	20	21	3.1	6.1	13
40	.31	.41	.47	.026	.032	.040	1.4	1.8	2.9	.080	.14	.22	10	22	26	2.0	2.5	3.6	17	19	20	2.2	4.3	7.9
60	.35	.40	.46	.012	.012	.016	1.4	1.8	2.8	.058	.073	.086	10	23	27	1.4	1.7	2.5	17	20	20	1.5	2.9	5.4

Thickness Interior Partition (psf)	Area 5						Areas 6 and 7						Area 8					
	Floor 1						Floor 1						Floor 1					
	Position A			Position B			Position A			Position B			Position A			Position B		
	2-1/2"	5"	7-1/2"	2-1/2"	5"	7-1/2"	2-1/2"	5"	7-1/2"	2-1/2"	5"	7-1/2"	2-1/2"	5"	7-1/2"	2-1/2"	5"	7-1/2"
0	26	27	28	26	27	27	15	14	13	15	14	14	3.5	3.1	2.8	3.5	3.0	2.8
20	24	25	26	17	18	18	14	13	12	10	9.4	9.5	3.4	3.0	2.5	2.4	2.0	1.8
40	23	24	23	11	11	12	13	12	11	6.2	5.8	5.8	3.0	2.7	2.4	1.4	1.3	1.1
60	23	25	24	6.8	7.3	7.3	13	12	12	4.4	3.8	3.8	3.2	2.8	2.5	1.0	.96	.77
	Floor 2						Floor 2						Floor 2					
0	26	27	27	27	28	27	14	14	14	14	14	14	2.7	2.8	2.8	2.7	2.8	2.7
20	24	26	25	18	18	18	13	13	13	9.2	9.4	9.3	2.5	2.6	2.5	1.7	1.8	1.8
40	23	24	24	11	12	12	12	12	12	5.6	5.9	5.9	2.3	2.5	2.4	1.1	1.1	1.1
60	24	25	24	6.7	7.2	7.0	13	13	13	3.7	3.9	3.8	2.4	2.6	2.5	.74	.78	.77
	Floor 3						Floor 3						Floor 3					
0	23	26	27	24	27	28	12	13	13	13	14	14	2.4	2.6	2.7	2.6	2.7	2.8
20	22	24	25	18	18	19	11	13	13	8.5	9.2	9.2	2.3	2.4	2.5	1.7	1.8	1.8
40	21	23	24	9.8	11	12	11	11	11	5.4	5.7	5.7	2.2	2.3	2.3	1.0	1.1	1.1
60	22	24	24	5.8	7.0	7.2	11	12	12	3.4	3.9	3.7	2.3	2.4	2.4	.67	.76	.75
	Floor 4						Floor 4						Floor 4					
0	20	25	27	16	27	27	11	14	14	13	14	14	2.3	2.7	2.7	2.6	2.8	2.8
20	21	24	25	11	18	18	11	13	13	8.4	9.4	9.5	2.3	2.5	2.6	1.7	1.8	1.8
40	20	23	24	7.2	11	11	11	12	12	5.1	5.9	5.9	2.3	2.4	2.4	1.0	1.1	1.1
60	21	23	24	5.0	7.2	7.2	11	12	13	3.5	4.0	3.9	2.3	2.5	2.5	.66	.75	.75
	Floor 5						Floor 5						Floor 5					
0	19	23	26	7.8	25	27	9.9	13	14	8.9	14	14	2.1	2.7	2.8	2.0	2.7	2.8
20	20	23	24	6.2	17	17	10	13	13	6.2	9.2	9.6	2.1	2.5	2.6	1.4	1.7	1.8
40	19	22	23	4.5	9.8	11	9.7	12	12	4.0	5.7	6.1	2.1	2.4	2.4	.85	1.1	1.1
60	20	23	24	3.3	6.5	7.0	10	13	13	2.7	3.7	3.9	2.2	2.5	2.5	.61	.75	.75
	Floor 6						Floor 6						Floor 6					
0	19	20	24	5.1	22	27	9.9	12	14	6.3	14	15	2.1	2.6	2.8	1.6	2.8	2.9
20	19	21	23	4.6	14	17	10	12	13	4.8	9.5	9.9	2.1	2.5	2.6	1.1	1.8	1.9
40	19	20	23	3.3	8.8	11	9.7	11	13	3.2	4.8	6.3	2.0	2.3	2.5	.71	1.1	1.2
60	19	21	23	2.4	5.7	7.0	10	12	13	2.2	3.7	4.0	2.1	2.5	2.5	.52	.75	.75

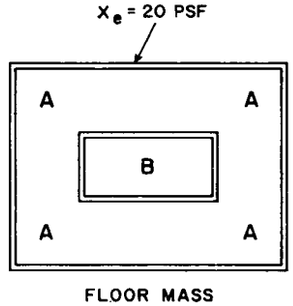

FLOOR MASS
THICKNESS = 80 PSF

TABLE 4

DOSE RATE IN MODEL BUILDING, CORRIDOR GEOMETRY
(r/hr normalized to source density of 1 curie/ft^2)

Thickness Interior Partition (psf)	Area 1												Area 2											
	Floor 1												Floor 1											
	Position A			Position B			Position D			Position F			Position A			Position B			Position D			Position F		
	2-1/2"	5"	7-1/2"	2-1/2"	5"	7-1/2"	2-1/2"	5"	7-1/2"	2-1/2"	5"	7-1/2"	2-1/2"	5"	7-1/2"	2-1/2"	5"	7-1/2"	2-1/2"	5"	7-1/2"	2-1/2"	5"	7-1/2"
0	49	51	46	26	34	40							34	34	32	31	30	32						
20	48	49	43	16	22	27	16	22	27	24	30	32	30	29	28	20	18	19	20	20	24	22	22	22
40	48	47	41	11	14	17	11	15	17	21	23	24	27	26	25	12	12	13	12	13	13	17	17	17
60	45	45	39	6.5	8.9	11	7.5	8.6	12	13	14	14	26	25	25	8.2	8.2	8.3	8.6	8.9	9.0	12	12	12
	Floor 2												Floor 2											
0	6.9	13	15	2.9	3.4	3.7							18	21	20	4.0	5.4	13						
20	6.4	12	15	1.7	1.9	2.1	1.9	2.1	2.5	3.0	4.3	5.5	17	20	20	2.3	4.2	8.7	2.3	4.7	9.8	4.8	10	13
40	6.5	12	14	1.2	1.3	1.4	1.4	1.6	1.9	2.4	3.9	4.6	17	19	19	1.5	2.6	5.5	1.3	3.6	7.2	4.3	8.3	5.0
60	6.4	12	14	.77	.73	.80	.84	.82	.94	1.7	2.2	2.9	15	19	18	1.0	1.8	3.5	.99	2.2	4.8	3.6	6.1	7.2
	Floor 3												Floor 3											
0	2.5	3.2	5.3	1.1	1.4	1.6							5.2	13	14	2.2	3.1	3.6						
20	2.4	3.1	4.7	.68	.77	.88	.77	.94	1.0	1.2	1.3	1.5	5.1	13	13	1.3	1.7	2.0	1.4	1.9	2.2	2.1	3.9	5.7
40	2.3	2.9	4.4	.44	.51	.51	.59	.59	.64	1.0	1.1	1.2	5.0	12	13	.92	1.1	1.3	1.1	1.2	1.5	1.8	3.7	5.2
60	2.3	3.0	4.7	.29	.29	.29	.36	.32	.37	.62	.64	.74	4.8	12	13	.68	.77	.88	.70	.74	.97	1.2	1.4	3.5
	Floor 4												Floor 4											
0	1.3	1.4	1.7	.69	.75	.93							3.3	6.3	8.3	1.5	1.9	2.2						
20	1.3	1.5	1.8	.23	.29	.35	.26	.29	.37	.49	.57	.61	3.0	6.2	8.8	.85	1.0	1.2	.97	1.1	1.3	1.4	1.9	2.9
40	1.2	1.3	1.6	.14	.16	.22	.18	.21	.27	.43	.45	.51	2.9	5.9	8.5	.62	.69	.75	.75	.84	.92	1.2	2.0	2.4
60	1.2	1.3	1.6	.078	.086	.098	.088	.098	.11	.23	.25	.27	2.9	6.1	8.7	.41	.43	.48	.50	.52	.54	1.0	1.5	2.2
	Floor 5												Floor 5											
0	.79	.90	.95	.16	.28	.36							1.9	2.8	4.4	.85	1.1	1.3						
20	.61	.70	.74	.10	.14	.14	.12	.16	.18	.24	.26	.31	2.1	2.9	4.7	.41	.54	.66	.51	.66	.74	.88	1.1	1.4
40	.58	.66	.70	.061	.070	.082	.057	.064	.072	.11	.12	.14	1.9	2.8	4.6	.33	.34	.45	.38	.47	.54	.81	1.0	1.3
60	.57	.68	.70	.036	.041	.043	.041	.045	.051	.088	.088	.088	1.9	2.9	4.7	.21	.22	.29	.28	.31	.34	.75	.90	1.1
	Floor 6												Floor 6											
0	.40	.48	.57	.16	.18	.18							1.4	1.8	2.8	.54	.67	.80						
20	.32	.40	.44	.053	.076	.073	.061	.067	.090	.12	.14	.17	1.4	1.7	2.6	.28	.36	.41	.29	.37	.43	.58	.69	.79
40	.30	.39	.43	.029	.037	.045	.039	.045	.053	.061	.072	.092	1.3	1.7	2.5	.17	.21	.26	.20	.26	.32	.47	.56	.68
60	.28	.34	.40	.018	.021	.023	.027	.027	.029	.037	.041	.047	1.3	1.7	2.6	.09	.11	.13	.13	.15	.19	.41	.45	.57

Thickness Interior Partition (psf)	Area 3												Area 4											
	Floor 1												Floor 1											
	Position A			Position B			Position D			Position F			Position A			Position B			Position D			Position F		
	2-1/2"	5"	7-1/2"	2-1/2"	5"	7-1/2"	2-1/2"	5"	7-1/2"	2-1/2"	5"	7-1/2"	2-1/2"	5"	7-1/2"	2-1/2"	5"	7-1/2"	2-1/2"	5"	7-1/2"	2-1/2"	5"	7-1/2"
0	62	64	64	61	63	63							29	29	29	29	29	30						
20	52	53	52	37	39	39	37	41	39	41	44	42	25	24	22	17	18	18	17	18	19	19	20	19
40	50	51	49	26	27	27	25	28	28	32	33	33	22	23	22	11	12	12	11	13	14	14	15	14
60	48	50	48	16	17	17	17	18	18	24	24	25	20	21	20	6.9	7.7	7.6	7.2	8.6	8.3	10	10	10
	Floor 2												Floor 2											
0	44	51	55	22	52	57							25	29	29	27	30	29						
20	45	47	48	16	32	35	17	34	38	27	38	38	24	24	22	16	18	18	16	18	18	17	19	19
40	44	46	46	11	21	23	12	23	25	20	27	27	21	22	22	11	12	11	10	12	14	12	14	14
60	43	44	34	7.1	14	15	8.5	15	16	15	21	20	20	21	21	6.6	7.6	7.5	6.9	8.0	8.5	9.5	10	9.8
	Floor 3												Floor 3											
0	37	42	45	12	25	42							21	25	28	14	28	30						
20	36	40	41	6.3	17	26	7.7	19	28	13	24	31	23	21	21	8.9	17	17	11	17	18	14	18	19
40	33	39	39	3.4	10	16	4.6	14	19	11	19	22	19	20	21	5.4	11	12	6.8	11	12	10	13	14
60	34	37	39	3.1	8.1	12	3.3	8.5	13	8.5	15	17	19	19	20	3.8	6.9	7.4	4.9	7.1	7.8	6.9	9.4	9.5
	Floor 4												Floor 4											
0	28	38	38	7.7	14	26							21	23	27	6.4	23	29						
20	27	36	36	4.5	7.9	16	4.7	9.2	17	8.2	16	22	21	21	20	4.3	14	17	4.5	15	17	9.8	17	18
40	25	34	35	3.0	5.1	9.5	3.2	5.9	11	7.0	12	17	20	20	20	3.0	8.9	11	3.5	9.6	11	7.4	12	13
60	26	34	35	1.9	3.8	7.1	2.3	3.4	7.9	3.1	11	13	18	19	19	2.0	5.9	7.0	2.3	6.3	7.3	6.0	8.8	9.0
	Floor 5												Floor 5											
0	17	30	33	6.6	7.9	13							20	21	23	4.4	14.	25						
20	17	30	31	3.5	4.4	8.0	3.8	4.9	10	5.7	12	16	20	20	18	3.2	9.0	15	3.6	12	15	8.1	14	16
40	16	28	30	2.4	3.1	5.3	2.6	3.5	6.7	4.4	9.2	13	18	19	19	2.2	5.7	9.5	2.4	7.5	9.5	6.3	10	12
60	16	29	30	1.6	1.9	3.4	1.7	2.3	4.7	3.9	7.9	9.5	17	18	18	1.5	3.9	6.2	1.6	4.9	8.2	5.2	7.3	8.2
	Floor 6												Floor 6											
0	12	24	28	4.3	5.7	8.5							18	20	21	4.2	8.6	21						
20	11	23	26	2.8	3.4	4.6	3.0	3.6	5.4	4.0	8.3	11	19	19	17	2.7	6.0	13	2.8	6.7	13	6.0	11	16
40	9.3	22	26	1.9	2.1	3.1	2.1	2.5	3.6	3.2	6.5	8.4	16	18	19	1.8	3.7	7.6	1.8	4.3	8.4	4.2	7.6	10
60	10	22	25	1.2	1.4	1.9	1.4	1.6	2.5	2.9	5.4	7.2	16	17	17	1.2	2.4	5.0	1.2	3.0	5.7	3.9	6.0	7.5

TABLE 4 (Cont'd.)

DOSE RATE IN MODEL BUILDING, CORRIDOR GEOMETRY
(r/hr normalized to source density of 1 curie/ft^2)

Thickness Interior Partition (psf)	Area 5												Areas 6 and 7											
	Floor 1												Floor 1											
	Position A			Position B			Position D			Position F			Position A			Position B			Position D			Position F		
	2-1/2"	5"	7-1/2"	2-1/2"	5"	7-1/2"	2-1/2"	5"	7-1/2"	2-1/2"	5"	7-1/2"	2-1/2"	5"	7-1/2"	2-1/2"	5"	7-1/2"	2-1/2"	5"	7-1/2"	2-1/2"	5"	7-1/2"
0	26	27	28	26	27	27							15	14	13	15	14	14						
20	21	22	21	15	16	17	15	16	17	17	18	18	13	12	12	9.4	9.4	8.8	9.4	8.5	8.8	11	10	9.7
40	20	21	20	10	11	11	11	11	11	13	13	13	11	11	11	6.3	5.9	5.9	6.4	6.0	6.0	7.4	7.2	6.9
60	19	21	20	7.2	7.7	7.7	7.8	8.3	9.9	9.4	9.9	9.9	10	9.4	9.4	4.2	4.1	4.0	4.4	4.3	4.2	5.5	5.2	5.2
	Floor 2												Floor 2											
0	26	27	27	27	28	27							14	14	14	14	14	14						
20	22	23	22	15	16	16	16	17	17	16	18	17	13	13	12	8.6	9.1	8.7	9.0	9.2	9.1	9.2	9.7	9.3
40	20	21	21	10	11	11	11	11	12	12	13	13	10	11	11	5.8	6.0	5.9	5.9	6.2	6.1	6.8	7.0	6.8
60	21	21	21	7.1	7.6	7.5	7.4	8.0	8.0	9.2	9.8	9.6	9.9	9.9	9.9	3.8	4.0	3.0	4.1	4.4	4.3	5.2	5.4	5.2
	Floor 3												Floor 3											
0	23	26	27	24	27	28							12	13	13	13	14	14						
20	20	21	21	14	17	17	15	17	17	16	17	18	11	11	11	7.8	8.7	8.7	8.3	8.8	9.0	8.7	9.5	9.5
40	19	20	22	9.0	11	11	9.7	11	12	12	13	13	9.1	9.9	9.9	5.1	5.9	5.9	5.6	6.1	6.1	6.3	6.9	6.9
60	18	20	20	6.0	7.4	7.6	7.8	9.1	9.2	7.8	8.7	9.2	8.5	9.2	9.5	3.4	3.9	4.0	3.9	4.1	4.2	4.8	5.1	5.3
	Floor 4												Floor 4											
0	20	25	27	16	27	27							11	14	14	13	14	14						
20	19	21	22	10	16	17	12	16	17	14	17	18	10	11	12	7.8	8.9	9.1	7.6	9.1	9.2	8.5	9.6	9.7
40	19	20	21	6.8	11	11	7.9	11	11	10	12	12	9.4	10	10	5.1	5.9	6.1	5.0	6.1	6.2	6.1	6.9	7.0
60	19	19	20	4.7	7.1	7.4	5.6	7.4	9.4	7.8	9.1	9.4	8.8	9.5	9.7	3.4	3.9	4.1	3.5	4.1	4.3	4.6	5.3	5.3
	Floor 5												Floor 5											
0	19	23	26	7.8	25	27							9.9	13	14	8.9	14	14						
20	19	20	21	5.2	16	16	6.3	16	17	11	16	17	10	11	12	6.2	8.8	8.9	7.3	9.2	9.2	8.4	9.5	9.7
40	18	19	20	4.0	10	11	4.7	10	11	8.7	12	13	9.1	10	11	4.0	5.9	6.2	4.9	6.3	6.4	6.1	7.0	7.3
60	18	19	20	2.7	6.8	7.3	3.4	6.9	7.5	6.4	8.8	9.2	8.5	9.6	9.8	2.7	3.9	4.0	3.3	4.2	4.3	4.4	5.1	5.3
	Floor 6												Floor 6											
0	19	20	24	5.1	22	27							9.9	12	14	6.3	14	15						
20	18	19	19	3.9	14	16	3.6	13	15	8.3	15	16	10	11	12	4.4	9.0	9.4	5.3	8.7	9.2	8.4	9.1	9.9
40	18	19	19	2.8	9.1	11	2.9	9.3	11	6.8	11	12	9.4	9.9	11	3.0	6.0	6.2	3.6	6.0	6.3	5.4	6.8	7.3
60	18	18	18	2.1	5.8	7.1	2.1	6.1	7.0	5.1	8.2	8.6	8.7	9.4	9.8	2.2	3.7	4.0	2.7	4.0	4.3	4.0	4.9	5.3

Thickness Interior Partition (psf)	Area 8											
	Floor 1											
	Position A			Position B			Position D					
	2-1/2"	5"	7-1/2"	2-1/2"	5"	7-1/2"	2-1/2"					
0	3.5	3.1	2.8	3.5	3.0	2.8						
20	3.0	2.7	2.3	2.4	2.3							1.9
40	2.7	2.4	2.2	1.7	1.9						1.6	1.4
60	2.6	2.4	2.1	1.1	.90	.8			.9	1.2	1.1	.96
						F						
0	2.7	2.8	2.8	2.7	2.8	2.7						
20	2.4	2.4	2.4	1.7	1.7	1.9		.8	1.8	1.8	1.8	1.8
40	2.2	2.2	2.2	1.1	1.2	1.3		1.2	1.2	1.3	1.4	1.4
60	2.1	2.2	2.1	.74	.77	.7		.1	.79	.91	.97	.96
						I						
0	2.4	2.6	2.7	2.6	2.7	2.8						
20	2.2	2.3	2.3	1.6	1.7	1		1.7	1.8	1.7	1.8	1.8
40	2.0	2.1	2.1	1.0	1.2	1.3	1	1.2	1.2	1.3	1.4	1.3
60	1.9	2.0	2.1	.67	.76		.74	.80	.79	.83	.92	.92
	Floor 4											
0	2.3	2.7	2.7	2.6	2.8	2.8						
20	2.2	2.3	2.3	1.6	1.7	1.8	1.5	1.7	1.7	1.7	1.8	1.9
40	2.0	2.1	2.2	1.1	1.2	1.2	1.1	1.2	1.2	1.2	1.4	1.4
60	2.0	2.0	2.0	.70	.77	.77	.68	.79	.79	.81	.94	.94
	Floor 5											
0	2.1	2.7	2.8	2.0	2.7	2.8						
20	2.1	2.3	2.3	1.4	1.7	1.7	1.4	1.8	1.8	1.6	1.8	1.8
40	2.0	2.2	2.2	.94	1.2	1.2	.97	1.2	1.2	1.2	1.4	1.4
60	1.9	2.1	2.1	.60	.74	.75	.61	.78	.79	.80	.92	.92
	Floor 6											
0	2.1	2.6	2.8	1.6	2.8	2.9						
20	2.0	2.2	2.3	1.1	1.7	1.8	1.3	1.6	1.8	1.5	1.8	1.9
40	2.0	2.1	2.2	.72	1.2	1.2	.87	1.2	1.2	1.1	1.3	1.3
60	1.9	2.1	2.2	.46	.74	.79	.56	.74	.79	.77	.93	.93

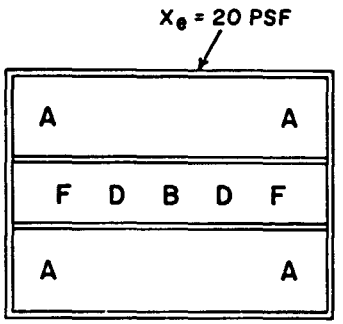

FLOOR MASS
THICKNESS = 80 PSF

TABLE 5

DOSE RATE IN MODEL BUILDING, COMPARTMENT GEOMETRY
(r/hr normalized to source density of 1 curie/ft^2)

Thickness Compartment (psf)	Position A			Position B			Position C			Position D			Position E			Position F			Position G		
Area 1																					
Floor 1																					
	2-1/2"	5"	7-1/2"	2-1/2"	5"	7-1/2"	2-1/2"	5"	7-1/2"	2-1/2"	5"	7-1/2"	2-1/2"	5"	7-1/2"	2-1/2"	5"	7-1/2"	2-1/2"	5"	7-1/2"
0	48	47	41	11	14	17				11	15	17				21	23	24			
10	40	41	36	8.3	11	12	7.3	9.4	10	9.1	12	13	12	15	16	17	19	18	30	28	25
20	42	41	36	7.0	9.5	11	7.1	9.2	9.8	8.0	11	11	11	13	15	15	17	17	29	27	24
40	42	41	36	6.6	8.5	9.6	5.8	7.3	8.0	6.7	9.0	9.4	10	12	13	15	17	16	29	27	23
Floor 3																					
0	2.3	2.9	4.4	.44	.51	.51				.59	.59	.64				1.0	1.1	1.2			
10	2.2	2.8	4.1	.38	.40	.42	.36	.40	.42	.44	.44	.49	.56	.60	.61	.83	.99	1.1	2.1	2.8	2.8
20	2.1	2.6	4.0	.32	.35	.37	.30	.34	.34	.40	.38	.42	.52	.56	.60	.74	.80	.90	1.9	2.6	2.5
40	2.1	2.6	3.9	.28	.31	.34	.27	.30	.30	.36	.32	.35	.48	.52	59	.66	.66	.66	1.1	1.6	1.9
Floor 5																					
0	.58	.66	.70	.061	.070	.082				.057	.064	.072				.11	.12	.14			
10	.56	.63	.67	.044	.048	.056	.052	.054	.058	.060	.063	.074	.071	.089	.11	.14	.17	.18	.35	.46	.51
20	.53	.59	.61	.040	.042	.044	.050	.052	.056	.057	.061	.072	.060	.060	.080	.12	.14	.14	.34	.42	.50
40	.50	.58	.61	.036	.040	.042	.050	.050	.052	.055	.059	.070	.056	.056	.080	.10	.11	.11	.26	.30	.36

Thickness Compartment (psf)	Position A			Position B			Position C			Position D			Position E			Position F			Position G		
Area 2																					
Floor 1																					
	2-1/2"	5"	7-1/2"	2-1/2"	5"	7-1/2"	2-1/2"	5"	7-1/2"	2-1/2"	5"	7-1/2"	2-1/2"	5"	7-1/2"	2-1/2"	5"	7-1/2"	2-1/2"	5"	7-1/2"
0	27	26	25	12	12	13				12	13	13				17	17	17			
10	26	25	25	9.6	9.6	10	9.6	9.7	9.7	9.6	10	10	12	12	14	14	14	14	18	18	17
20	25	24	23	9.0	9.2	9.5	7.9	8.3	8.2	8.5	9.0	8.8	11	11	11	13	13	13	17	17	16
40	23	23	22	8.0	8.1	8.4	6.8	7.0	6.9	7.4	7.7	7.5	10	10	10	12	12	12	17	17	16
Floor 3																					
0	5.0	12	13	.92	1.1	1.3				1.1	1.2	1.5				1.8	3.7	5.2			
10	5.3	12	13	.66	.77	.89	.75	.86	.97	.80	.95	1.1	1.1	1.3	2.6	1.3	2.5	3.7	5.3	6.5	6.3
20	4.5	12	13	.66	.84	.97	.68	.79	.92	.77	.90	1.1	1.0	1.2	2.1	1.4	2.9	3.7	5.1	6.5	6.0
40	4.5	11	12	.48	.57	.66	.33	.35	.44	.44	.48	.57	.62	.68	.79	.86	1.4	2.2	2.2	4.3	4.6
Floor 5																					
0	1.9	2.8	4.6	.33	.34	.45				.39	.47	.54				.81	1.0	1.3			
10	2.1	2.9	5.0	.20	.24	.29	.23	.29	.33	.31	.35	.40	.41	.46	.54	.54	.63	.81	1.4	2.4	2.7
20	1.8	2.5	4.2	.21	.29	.33	.21	.29	.31	.26	.33	.40	.37	.46	.53	.62	.73	1.0	1.7	2.6	2.8
40	1.8	2.5	4.2	.18	.22	.26	.19	.20	.24	.24	.26	.33	.37	.40	.46	.51	.59	.75	1.0	2.0	2.3

Thickness Compartment (psf)	Area 3																				
	Floor 1																				
	Position A			Position B			Position C			Position D			Position E			Position F			Position G		
	2-1/2"	5"	7-1/2"	2-1/2"	5"	7-1/2"	2-1/2"	5"	7-1/2"	2-1/2"	5"	7-1/2"	2-1/2"	5"	7-1/2"	2-1/2"	5"	7-1/2"	2-1/2"	5"	7-1/2"
0	50	51	49	26	27	27				25	28	28				32	33	33			
10	47	49	48	20	22	23	20	22	21	19	22	22	24	25	25	27	29	28	35	37	34
20	44	45	44	19	20	21	17	19	18	17	20	19	23	24	24	24	26	25	32	33	32
40	40	43	43	20	16	16	14	16	15	14	17	17	20	21	22	22	25	24	31	33	32
	Floor 3																				
0	33	39	39	3.4	10	16				4.6	14	19				11	19	22			
10	33	38	39	3.8	9.3	14	3.8	8.8	13	3.8	10	15	5.4	14	18	10	17	20	23	25	27
20	32	36	37	3.7	9.2	13	3.4	8.7	12	3.7	9.0	13	5.4	13	17	10	16	19	20	24	25
40	32	35	35	2.9	7.9	12	2.9	7.0	10	3.2	7.9	11	4.5	12	16	8.4	15	17	19	22	23
	Floor 5																				
0	16	28	30	2.4	3.1	5.3				2.6	3.5	6.7				4.4	9.2	13			
10	16	28	30	2.1	2.4	4.5	2.0	2.5	4.7	2.3	2.6	5.7	2.6	4.4	7.7	4.2	8.2	11	14	16	17
20	15	27	29	1.9	2.3	4.0	1.8	2.4	4.1	2.0	2.6	5.1	2.5	4.2	7.6	4.6	8.8	11	14	15	16
40	15	28	29	1.7	2.0	3.6	1.6	2.1	3.9	1.9	2.5	5.0	2.5	4.2	7.4	3.9	8.2	11	13	15	16

Thickness Compartment (psf)	Area 4																				
	Floor 1																				
	Position A			Position B			Position C			Position D			Position E			Position F			Position G		
	2-1/2"	5"	7-1/2"	2-1/2"	5"	7-1/2"	2-1/2"	5"	7-1/2"	2-1/2"	5"	7-1/2"	2-1/2"	5"	7-1/2"	2-1/2"	5"	7-1/2"	2-1/2"	5"	7-1/2"
0	22	23	22	11	12	12				11	13	14				14	15	14			
10	20	22	21	9.3	10	10	9.3	10	9.6	9.2	10	9.8	11	11	12	12	13	12	15	16	15
20	19	21	20	8.9	9.7	9.7	8.1	8.8	8.6	8.5	9.2	8.9	11	11	12	11	12	11	14	15	15
40	19	20	20	7.3	8.2	8.4	7.0	7.9	8.0	6.9	7.9	7.8	9.5	10	11	11	12	12	14	15	15
	Floor 3																				
0	19	20	21	5.4	11	12				6.8	11	12				10	13	14			
10	19	20	20	5.3	10	10	5.4	9.3	10	6.2	9.4	10	7.7	11	11	9.5	12	12	13	14	15
20	19	20	20	4.8	8.9	9.0	4.8	7.6	8.0	5.4	8.2	8.7	7.6	10	11	9.0	11	11	13	14	14
40	18	19	19	3.9	7.2	7.3	4.2	6.8	6.9	4.9	7.2	7.8	6.7	8.9	9.2	8.3	10	10	12	14	13
	Floor 5																				
0	18	19	19	2.2	5.7	9.5				2.4	7.5	9.5				6.3	10	12			
10	17	19	19	2.0	5.4	8.3	2.0	5.7	8.1	2.1	6.3	8.1	2.9	7.9	9.4	6.0	9.2	11	10	12	13
20	17	19	19	1.8	4.8	7.4	1.8	4.8	6.8	2.1	5.8	7.4	3.1	7.7	9.3	6.2	9.2	10	10	12	13
40	17	18	18	1.6	4.5	6.9	1.6	4.1	6.1	1.7	5.4	6.9	2.6	7.3	8.8	5.9	8.8	9.8	9.9	12	13

TABLE 5 (Cont'd.)

DOSE RATE IN MODEL BUILDING, COMPARTMENT GEOMETRY
(r/hr normalized to source density of 1 curie/ft^2)

Thickness Compartment (psf)	Area 5																				
	Floor 1																				
	Position A			Position B			Position C			Position D			Position E			Position F			Position G		
	2-1/2"	5"	7-1/2"	2-1/2"	5"	7-1/2"	2-1/2"	5"	7-1/2"	2-1/2"	5"	7-1/2"	2-1/2"	5"	7-1/2"	2-1/2"	5"	7-1/2"	2-1/2"	5"	7-1/2"
0	20	21	20	10	11	11				11	11	11				13	13	13			
10	19	20	19	8.6	9.4	9.3	8.6	9.3	8.9	8.5	9.5	9.3	10	11	11	11	12	11	14	15	14
20	18	20	19	8.5	9.7	9.5	8.1	8.8	8.2	8.1	8.6	8.4	10	11	11	11	11	11	14	15	14
40	17	19	19	6.6	7.3	7.4	6.2	7.1	7.2	6.2	7.6	7.4	8.4	9.1	9.9	10	10	10	13	14	14
	Floor 3																				
0	19	20	22	9.0	11	11				9.7	11	12				12	13	13			
10	18	19	20	8.0	9.9	9.8	7.4	9.0	9.3	7.7	9.4	9.9	8.9	11	11	10	12	12	13	14	13
20	18	19	19	7.3	8.8	9.0	6.7	8.2	8.0	7.0	8.3	9.0	8.9	10	10	9.8	11	11	14	14	14
40	17	18	18	5.5	6.7	6.7	5.5	6.7	6.5	5.9	6.8	7.3	6.9	8.4	8.4	8.5	9.6	9.7	12	13	13
	Floor 5																				
0	18	19	20	4.0	10	11				4.7	10	11				8.7	12	13			
10	18	19	19	3.1	8.3	9.2	3.3	8.1	8.9	4.0	8.7	9.9	5.8	9.4	10	7.5	11	11	11	13	14
20	18	18	19	3.5	8.2	8.7	3.2	7.4	8.1	3.9	7.9	8.9	5.5	9.5	10	7.6	10	11	11	13	13
40	17	18	18	2.5	6.7	7.0	2.5	6.0	6.5	3.3	6.6	7.1	5.1	8.2	8.6	7.1	9.3	9.7	11	13	13

Thickness Compartment (psf)	Areas 6 and 7																				
	Floor 1																				
	Position A			Position B			Position C			Position D			Position E			Position F			Position G		
	2-1/2"	5"	7-1/2"	2-1/2"	5"	7-1/2"	2-1/2"	5"	7-1/2"	2-1/2"	5"	7-1/2"	2-1/2"	5"	7-1/2"	2-1/2"	5"	7-1/2"	2-1/2"	5"	7-1/2"
0	11	11	11	6.3	5.9	5.9				6.4	6.0	6.0				7.4	7.2	6.9			
10	10	9.4	9.3	5.1	4.9	4.9	5.1	4.8	4.6	5.1	4.7	4.6	6.1	5.6	4.6	6.1	6.0	5.8	7.4	7.3	7.3
20	11	10	10	5.4	5.1	5.0	4.8	4.6	4.3	4.6	4.8	4.5	6.2	6.0	6.1	6.4	6.1	6.1	7.8	7.8	7.4
40	10	9.7	9.4	4.6	4.4	4.2	4.5	4.3	4.0	4.2	4.4	4.2	5.6	5.3	5.3	5.8	5.8	5.6	7.6	7.1	7.4
	Floor 3																				
0	9.1	9.9	9.9	5.1	5.9	5.9				5.6	6.1	6.1				6.3	6.9	6.9			
10	8.7	9.1	9.0	4.3	5.0	4.9	4.1	4.8	4.8	4.7	4.9	5.0	5.0	5.6	5.4	5.5	5.9	5.9	6.7	7.3	6.9
20	9.5	9.7	9.7	4.3	4.8	4.8	4.2	4.3	4.2	4.2	4.3	4.8	5.0	5.6	5.5	5.2	5.7	5.6	6.7	7.3	7.0
40	9.1	9.4	9.4	3.9	4.6	4.6	3.6	3.9	3.9	4.1	4.3	4.5	4.9	5.3	5.3	5.0	5.6	5.5	6.7	7.3	6.7
	Floor 5																				
0	9.1	10	11	4.0	5.9	6.2				4.9	6.3	6.4				6.1	7.0	7.3			
10	9.0	9.5	9.6	3.7	4.8	5.1	3.4	4.6	4.9	3.9	4.9	5.0	4.4	5.4	5.7	5.1	5.9	5.9	6.5	6.8	7.0
20	9.7	10	10	3.6	4.9	4.9	3.4	4.6	4.8	3.9	4.9	4.9	4.6	5.6	5.7	5.2	6.2	6.2	6.9	7.3	7.6
40	9.7	9.8	9.9	3.4	4.5	4.5	3.3	4.3	4.5	3.8	4.6	4.6	4.5	5.5	5.3	5.3	6.0	6.2	7.0	7.3	7.4

Thickness Compartment (psf)	Area 8																				
	Floor 1																				
	Position A			Position B			Position C			Position D			Position E			Position F			Position G		
	2-1/2"	5"	7-1/2"	2-1/2"	5"	7-1/2"	2-1/2"	5"	7-1/2"	2-1/2"	5"	7-1/2"	2-1/2"	5"	7-1/2"	2-1/2"	5"	7-1/2"	2-1/2"	5"	7-1/2"
0	2.7	2.4	2.2	1.7	1.4	1.2				1.6	1.4	1.2				1.7	1.6	1.4			
10	2.5	2.3	2.1	1.3	1.2	1.0	1.3	1.1	.96	1.3	1.1	.98	1.5	1.3	1.2	1.5	1.3	1.2	1.8	1.7	1.5
20	2.5	2.2	2.1	1.3	1.1	1.0	1.2	1.0	.86	1.1	1.0	.90	1.6	1.3	1.2	1.4	1.3	1.2	1.7	1.6	1.5
40	2.5	2.2	2.0	1.2	1.0	.90	1.0	.84	.77	1.0	.92	.80	1.5	1.3	1.1	1.3	1.2	1.1	1.6	1.6	1.4
	Floor 3																				
0	2.0	2.1	2.1	1.0	1.2	1.2				1.1	1.2	1.2				1.3	1.4	1.3			
10	1.9	1.9	1.9	.87	.98	.96	.84	.94	.94	.90	.98	.99	.99	1.2	1.1	1.1	1.2	1.2	1.4	1.5	1.4
20	1.9	1.9	1.9	.82	.91	.91	.72	.84	.82	.84	.89	.89	.96	1.1	1.1	1.0	1.1	1.1	1.4	1.5	1.4
40	1.8	1.9	1.9	.82	.86	.86	.67	.72	.72	.74	.77	.79	.96	1.0	1.0	1.0	1.1	1.0	1.4	1.4	1.3
	Floor 5																				
0	2.0	2.2	2.2	.94	1.2	1.2				.97	1.2	1.2				1.2	1.4	1.4			
10	1.9	2.0	2.0	.87	.96	.99	.74	.94	.96	.79	.97	1.0	.89	1.1	1.1	1.0	1.2	1.2	1.4	1.4	1.5
20	1.9	2.0	2.0	.77	.91	.91	.65	.84	.86	.72	.91	.91	.89	1.1	1.1	1.0	1.2	1.2	1.4	1.5	1.5
40	1.9	2.0	1.9	.72	.86	.86	.60	.74	.74	.67	.84	.84	.89	1.0	1.1	.96	1.1	1.1	1.3	1.5	1.5

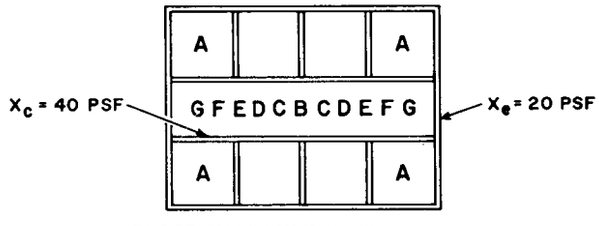

FLOOR MASS THICKNESS = 80 PSF

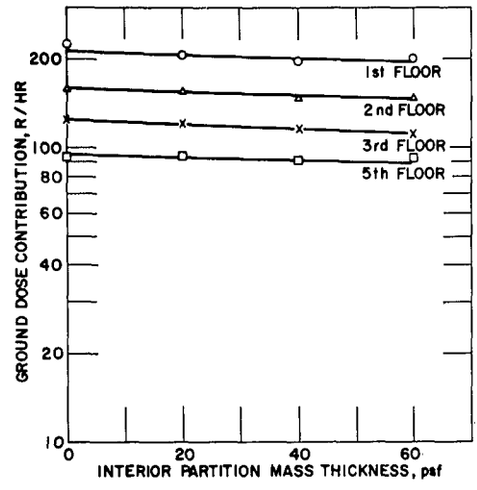

a. Box Partition, Detector Position A

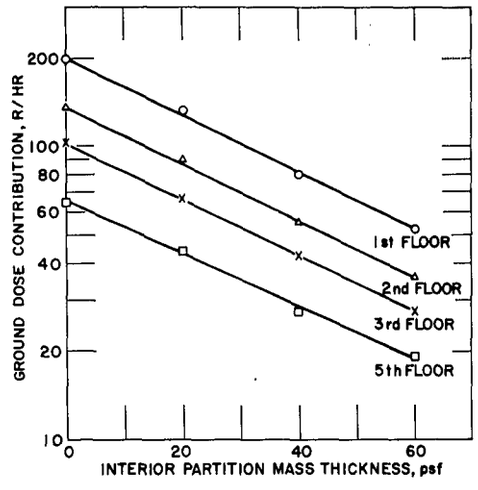

b. Box Partition, Detector Position B

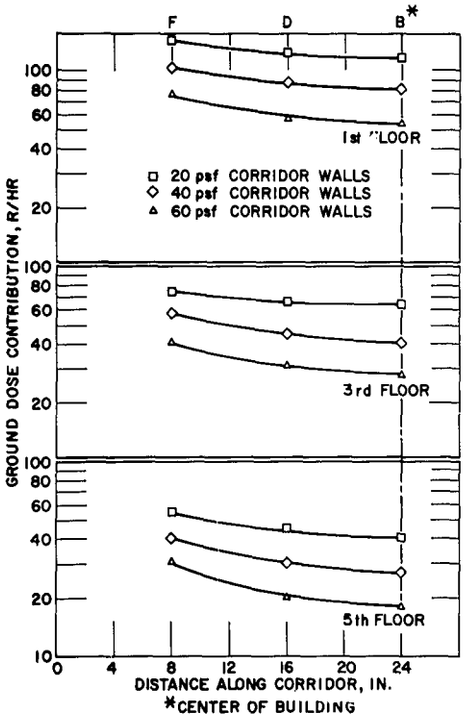

c. Corridor Geometry

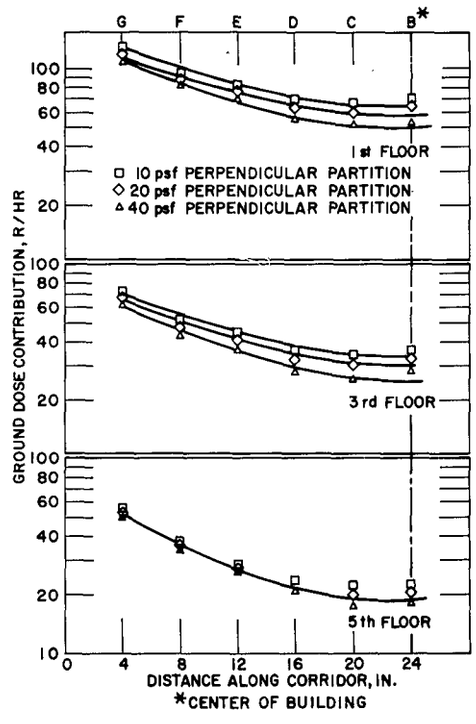

d. Compartment Geometry

Figure 6. Typical Measured Dose Rates for Partition Geometries at Mid-Floor Detector Heights (50 ft radius source field)

CHAPTER 3

ANALYSIS OF DATA

INTRODUCTION

Theoretical calculations of radiation protection afforded by existing complex structures have been simplified to the point where technical personnel, though not directly trained in the field of radiation physics, may make routine calculations based upon the building dimensions to determine the shielding factors of different locations within the building. Many assumptions had to be made to simplify the analytical procedures. The purpose of this study has been to evaluate the computational procedures set forth in the manual entitled "Design and Review of Structures for Protection from Fallout Gamma Radiation"[1] (hereafter called the Engineering Manual) as to their degree of accuracy for estimating the effect of interior partitions on the distribution of dose rate from ground-based fallout surrounding a multistory structure.

Experimental measurements have been made to verify and provide the basis for refinement of the computational procedures of the Engineering Manual for estimating the dose rate in a compartmentalized structure. Comparisons are made between experimentally determined dose rates and those determined from the computational procedure.

CONVERSION OF MODEL DATA TO FULL-SCALE DATA

Shielding results obtained from experimentation on model structures may be considered to be exact replicas of full-scale experiments if three basic laws of scaling are obeyed:

1. All dimensions must be scaled geometrically by the same factor.
2. Each absorbing surface must attenuate radiation to the same degree as the original surface independent of scaling factor.
3. The specific scattering and absorption factors must remain unchanged.

The principal difficulties lie in the interpretation of experimental evidence obtained on model structures arising from the third scaling rule. First, to increase the density of the building materials, the model is constructed of iron while the attenuation curves presented in the Engineering Manual have been computed for material with the scattering and absorption properties of water. Since an accurate reproduction of the relative scattering and absorption properties at all applicable radiation energies is required, there is some ambiguity in selecting the criteria for computing model wall thicknesses. Three points of comparison to full-scale walls can be made:

1. Mass thickness may be matched.
2. Broad-beam absorption data for flat slabs can be applied.
3. Electron density may be maintained.

To illustrate these points, we observe that a wall of iron 20 psf thick is equivalent to:

1. A wall of water 20 psf thick if criterion No. 1 is accepted
2. A wall of water 29 psf thick if criterion No. 2 is accepted
3. A wall of water 16.8 psf thick if criterion No. 3 is accepted.

A second ramification of the third scaling rule arises during consideration of modeling of the atmosphere and ground. It is difficult, if not impossible, to increase the density of the atmosphere and ground in a practical way to the extent required for perfect scaling. Results obtained from model tests must therefore be treated analytically to correct for this density difference artificially. Perhaps the most straightforward method of computing the effect of unscaled atmospheric density is as follows. The attenuation of radiation reaching a detector is a function of the geometry and mass thickness of the structure and the attenuation and scattering properties of the atmosphere. Since the model is assumed to represent accurately the full-scale structure in geometry and mass thickness, the difference between model and full-scale results is a function only of the ratio of the scattering and attenuation properties of the real and "model" atmosphere.

The scattering and attenuation properties of the atmosphere for cobalt radiation have been experimentally measured in many investigations.[11,12,13] The data, in

general, may be expressed by an analytical expression of the form:

$$I = I_o \frac{e^{-\mu r}}{r^2} \left[1 + a_1(\mu r) + a_2(\mu r)^2 + \ldots\right] \quad (1)$$

where

I_o = dose rate at a unit distance for a source

r = distance from the source

μ = total cross section

$\left[1 + a_1(\mu r) + a_2(\mu r)^2 + \ldots\right]$ = dose buildup factor

$a_1, a_2, a_3 \ldots$ = experimentally measured constants.

Various investigators have evaluated the constant a_1 as varying from about 0.55 several feet above the ground-air interface to about 1.0 at altitudes of 50 feet or more for values of $\mu r \geq 0.1$. A more exact analytical fit of the data may be obtained by adding terms of the form $a_n(\mu r)^n$. However, since in general these buildup factors have been measured over paths essentially parallel to the ground and, in radiation penetrating a structure, the radiation predominantly traverses angular paths, the increase in accuracy obtained in computing the ratio of model to full-scale results using additional terms is unwarranted in view of the lack of accuracy of angular buildup data and the increased complexity of computation required.

This representation of dose-buildup factor is admittedly crude; however, it is probably adequate as a ratio to compare model with full-scale experiments. The major problems that have arisen from use of this approximation are attributable to its poor representation of the scattered portions of the dose at small distances ($\mu r \leq 0.1$). As shown below, however, the actual ratio that must be computed to compare data obtained from a model with those obtained from a full-scale structure is that of total dose from a full-scale annular contaminated field to that from the corresponding model field. Thus, for close-in field locations, while the dose due to scattered radiation may be seriously in error, it is but a few per cent of the total dose for both model and full-scale conditions. Hence, the ratio may be accepted as valid.

The total dose arriving at a position located in a structure at the center of a contaminated annular area with radii r_i, r_o (see Figure 7) may be written as:

$$D\left(h, r_i \rightarrow r_o\right) = I_o G\left(X_e, h, a, b \ldots\right) \int_{r=r_i}^{r=r_o} \frac{2\pi\sigma B\left(\mu\sqrt{r^2+h^2}\right) e^{-\mu\sqrt{\left(r^2+h^2\right)}} r\,dr}{\left(r^2+h^2\right)} \quad (2)$$

where

$D\left(h, r, \rightarrow r_o\right)$ = dose rate at detector position of interest

h = detector height

r_i = inner radius of contaminated annulus

r_o = outer radius of contaminated annulus

I_o = dose rate at a unit distance from a 1-curie source

$G\left(X_e, h, a, b \ldots\right)$ = geometric and barrier shielding introduced by the structure at height h

X_e, a, b = barrier thickness and geometric factors describing the structure

σ = source density in curies per unit area

$B\left(\mu\sqrt{r^2+h^2}\right)$ = air buildup factor $\cong 1 + 0.55\mu\sqrt{r^2+h^2}$

μ = total linear coefficient for air = $(1/445)\text{ft}^{-1}$ for Co-60

which upon integration reduces to:

$$D\left(h, r_i \rightarrow r_o\right) = 2\pi\sigma I_o G\left(X_e, h, a, b \ldots\right) \left[E_1\left(\mu\rho_i\right) + 0.55e^{-\mu\rho_i} - E_1\left(\mu\rho_o\right) - 0.55e^{-\mu\rho_o}\right] \quad (3)$$

where

$$\rho_i = \sqrt{r^2 + h^2}$$

$$\rho_o = \sqrt{r_o^2 + h^2}$$

$$E_1(x) = \int_x^\infty \frac{e^{-t}}{t} dt.$$

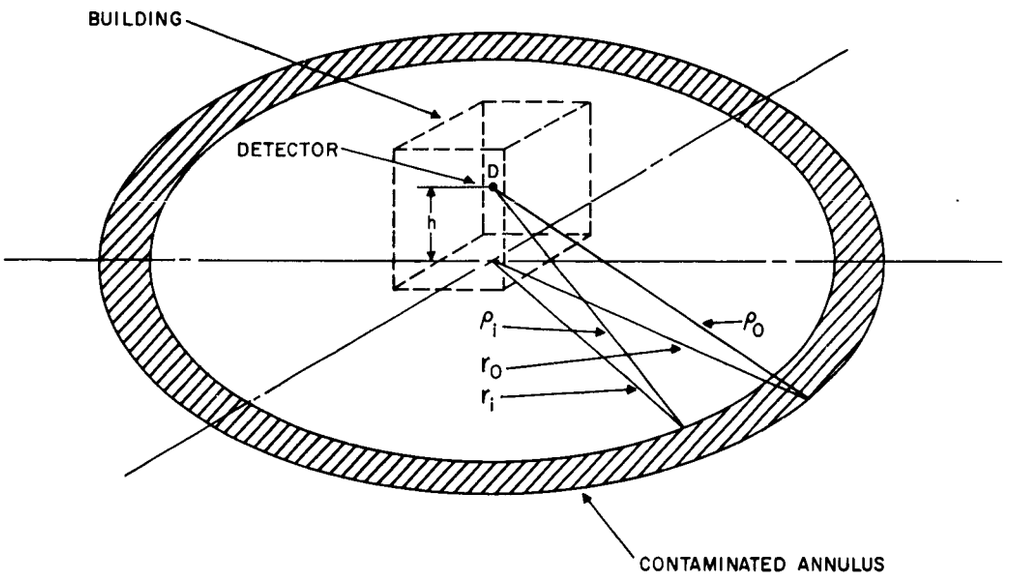

Figure 7. Schematic Diagram of Building Irradiated by an Annular Contaminated Field

The dose rate for the model and full-scale structure are both represented by the equation given above. Thus, if we take as the dimensions of interest the actual dimensions for the model, the corresponding equation for the full-scale structure would simply have each linear dimension multiplied by the scale factor "S." If the model structure is assumed to represent a 1/12-scale model (S = 12) of an actual

structure, the ratio of the dose that would be obtained from a full-scale test to that of the model test may be written as:

$$R = \frac{D_{FS}\left(h, r_i \rightarrow r_o\right)}{D_M\left(h, r_i \rightarrow r_o\right)} = \frac{E_1\left(12\mu\rho_i\right) - E_1\left(12\mu\rho_o\right) + 0.55\left[e^{-12\mu\rho_i} - e^{-12\mu\rho_o}\right]}{E_1\left(\mu\rho_i\right) - E_1\left(\mu\rho_o\right) + 0.55\left[e^{-\mu\rho_i} - e^{-\mu\rho_o}\right]} \quad (4)$$

where

$D_{FS}\ h, r_i \rightarrow r_o$ = dose that would be measured in a full-scale building

$D_M\ h, r_i \rightarrow r_o$ = dose as measured in the model structure

ρ_i, ρ_o = actual model source-area dimensions.

The data obtained from model experiments may then be multiplied by this ratio to obtain values that would have been obtained from a full-scale experiment. Table 6 presents the values (R) for the areas of interest.

TABLE 6

RATIO OF FULL-SCALE TO MODEL RESULTS

Source Area (See Figure 3)	Model Radii (ft)		Detector Height in Model (ft)					
	r_i	r_o	1/2	1-1/2	2-1/2	3-1/2	4-1/2	5-1/2
1	1.95	4.22	0.95	0.95	0.95	0.95	0.95	0.93
2	4.22	6.46	.94	.94	.93	.92	.92	.91
3	6.46	15.5	.88	.88	.88	.87	.87	.87
4	15.5	24.6	.78	.77	.77	.77	.77	.77
5	24.6	38.0	.66	.66	.66	.66	.65	.65
6,7	38.0	47.6	.54	.54	.54	.54	.54	.54
8	47.6	50.1	.48	.48	.48	.48	.48	.48

ESTIMATE OF FAR-FIELD RADIATION

It is of interest to estimate the additional amount of radiation that would have been obtained if the contaminated field had been simulated to an infinite radius. Referring to Eq. (3) for the dose rate from an annular area, we may write the approximate far-field fraction, in terms of the model, as the ratio of the dose from radiation originating beyond the outer radius used in the experiment to the dose originating from a certain annular source area. This annular area is located at a distance from the structure where the angular distribution of radiation striking the structure from the annulus is essentially the same as that which would arise from sources located at large distances from the structure:

$$\frac{D_M\left(r_o \rightarrow \infty\right)}{D_M\left(r_i \rightarrow r_o\right)} = \frac{E_1\left(\mu\rho_o\right) + 0.55\, e^{-\mu\rho_o}}{E_1\left(\mu\rho_i\right) - E_1\left(\mu\rho_o\right) + 0.55\left(e^{-\mu\rho_i} - e^{-\mu\rho_o}\right)} \qquad (5)$$

where

ρ_o = slant distance from detector to maximum outer radius of the outer field simulated

ρ_i = slant distance to the inner radius of the outer field simulated.

In a similar fashion the actual far-field dose to be expected from a full-scale structure may be estimated if the dose rate from an outlying contaminated annulus is known. In the present study, however, since only a model experiment has been performed, we must estimate this contribution from the outer annulus of the model experiment. As shown in Equation (4) and Table 6, the ratio of full-scale dose to model dose for the outer annulus is about 0.48 (Area 8). Thus, if the scale factor "S" is assumed to be 12, the far-field dose rate in the full-size structure may be

written in terms of the experimentally obtained dose from the outer model annulus and the model dimension as:

$$D_{FS}(r_o \rightarrow \infty) = D_M(r_i \rightarrow r_o)\left[\frac{D_{FS}(r_o \rightarrow \infty)}{D_M(r_i \rightarrow r_o)}\right]$$

$$= D_M(r_i \rightarrow r_o)\left[\frac{E_1(12\mu\rho_o) + 0.55e^{-12\mu\rho_o}}{E_1(\mu\rho_i) - E_1(\mu\rho_o) + 0.55\left(e^{-\mu\rho_i} - e^{-\mu\rho_o}\right)}\right] \quad (6)$$

where

$D_M(r_i \rightarrow r_o)$ = dose obtained experimentally from the outer annulus surrounding the model

$D_{FS}(r_o \rightarrow \infty)$ = dose that would be obtained from contamination existing beyond the outer radius of a full-scale structure

ρ_i = model slant distance from the detector location to the inner radius of the outer contaminated annulus

ρ_o = model slant distance from the detector location to the outer radius of the outer contaminated annulus.

The resultant ratio of full-scale far-field dose to outer-annulus model dose and the actual far-field dose expected is shown in Table 7.

TABLE 7

FAR-FIELD CORRECTIONS

Dosimeter Height in Model (ft)	Ratio of Full-Scale Far-Field Dose to Dose from Outer Annulus of Model
1/2	5.5
1-1/2	5.5
2-1/2	5.6
3-1/2	5.6
4-1/2	5.7
5-1/2	5.8

COMPUTATION OF FULL-SCALE VERSION OF MODEL BUILDING

The shielding calculations in the Engineering Manual are based upon 1-hour fallout spectra, while model results were obtained by using cobalt-60 as a fallout simulant. However, Spencer[14] presents curves of cobalt-60 attenuation and of fallout spectra for contamination adjacent to a vertical barrier, adjacent to a horizontal barrier, and on a horizontal barrier. The curves for fallout and cobalt-60 attenuation for thin exterior walls (20 psf) are for all practical purposes identical; therefore, since this is the case of interest, a direct comparison can be made between experiment and theory based on either the cobalt or fallout energy spectra.

The Engineering Manual method of computing the dose expected from ground sources of radiation in the center of a multistory, windowless structure without interior partitions is to divide the total radiation contribution into seven separate components (depending upon the mode of travel of the radiation to the detector), compute each of these components separately, and then add their sum. For a structure with no interior partitions, the equations required to determine these components for an infinite field of contamination using the terminology of Ref. 1 are given below (see Figure 8).

Skyshine radiation penetrating to the detector through the ceiling above the detector:

$$D_{ss}^{U} = \left[G_a(\omega'_u) - G_a(\omega_u) \right] (1 - S_w) B_w(X_e, H_u) B'_o(X_f)$$

Skyshine radiation penetrating to the detector through the walls of the same story as the detector:

$$D_{ss} = G_a(\omega_u)(1 - S_w) B_w(X_e, H)$$

Wall-scattered radiation from the story above the detector:

$$D_{ws}^{U} = \left[G_s(\omega'_u) - G_s(\omega_u) \right] S_w E B_w(X_e, H_u) B'_o(X_f)$$

Wall-scattered radiation from the walls of the same story as the detector:

$$D_{ws} = \left[G_s(\omega_u) + G_s(\omega_\ell)\right] S_w E B_w(X_e, H)$$

Wall-scattered radiation from the story below the detector:

$$D_{ws}^{L} = \left[G_s(\omega'_\ell) - G_s(\omega_\ell)\right] S_w E B_w(X_e, H_L) B_o(X_f)$$

Direct radiation from the same story as the detector:

$$D_d = \left[G_d(\omega_\ell, H)\right] (1 - S_w) B_w(X_e, H)$$

Direct radiation from the story below the detector:

$$D_d^{L} = \left[G_d(\omega'_\ell H) - G_d(\omega_\ell, H)\right] (1 - S_w) B_w(X_e, H) B_o(X_f)$$

where

$G_a(\omega)$ = the directional response of atmospheric-scattered radiation

$G_s(\omega)$ = the directional response of wall-scattered radiation

$G_d(\omega, H)$ = the directional response of direct radiation

ω = a solid angle fraction (solid angle/2π)(see Figure 8)

H = detector height above ground

H_u = mid-height of floor above detector

H_L = mid-height of floor below detector

S_w = the fraction of radiation scattered by the wall

E = an eccentricity factor depending upon length-to-width ratio

$B_w(X_e, H)$ = the barrier shielding introduced by a vertical wall of thickness X_e at height H above the ground

$B'_o(X_f)$ = the barrier shielding introduced by an overhead mass of thickness X_f to atmospheric or wall-scattered radiation

$B_o(X_f)$ = the barrier shielding introduced by a barrier of thickness X_f parallel to the field of contamination between the detector and the field.

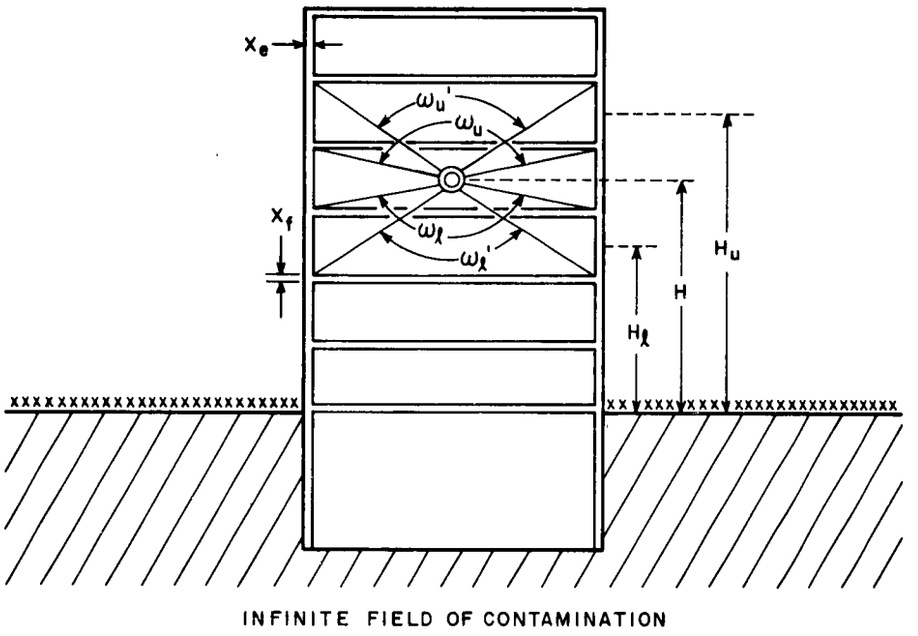

Figure 8. Application of Geometric Terminology of Engineering Manual to a Multistory Building

The simplest situation involving compartmentalized structures is called the box partition (or parallel partition) and is illustrated in Figure 1a. Each interior partition is parallel to a corresponding exterior partition. The Engineering Manual procedure for taking into account ground contribution that passes through interior parallel partitions to the center of the structure requires the calculation of the structure without interior partitions by the method outlined above, and then multiplying the ground contribution by a barrier factor that is a function of the mass thickness of the interior wall. The barrier factor for the interior wall is always taken at the 3-foot height because the height correction is already included in the barrier factor for the exterior wall. Thus the total dose arriving at a position located in the center of the structure is

$$D_T^* = D_T B_w\left(X_i, 3'\right)$$

where

D_T^* = total dose rate

D_T = dose rate in the center of structure without partitions

$B_w\left(X_i, 3'\right)$ = barrier factor for interior partitions (Ref. 1, Case 2, Chart 1).

The corner positions were calculated using the Engineering Manual's "position variation" procedure. The basic idea of this procedure is to divide the building into four quadrants (see Figure 9a), and to calculate the ground contribution for each quadrant by assuming that the detector is at the center of a fictitious structure just 4 times the size of each quadrant. Add the total contribution for all four fictitious structures and divide the sum by 4.

When interior partitions are present in the building, the corner position is calculated by using the azimuthal sector method in conjunction with the position variation procedure. Figure 9b shows a plan view of the building with interior partitions. On the basis of a structure with no interior partitions, the corner position is first computed as described above. The interior partitions lie within the third quadrant; therefore, this is the only quadrant affected by the partitions. Direct radiation entering through this third quadrant and integrated by the detector through azimuthal sectors A_{z_1} and A_{z_3} is shielded by the exterior wall only, while that entering sector A_{z_2} must also penetrate a double thickness of the interior partition. This portion of the radiation is thus attenuated by a barrier of twice the thickness of the interior partitions.

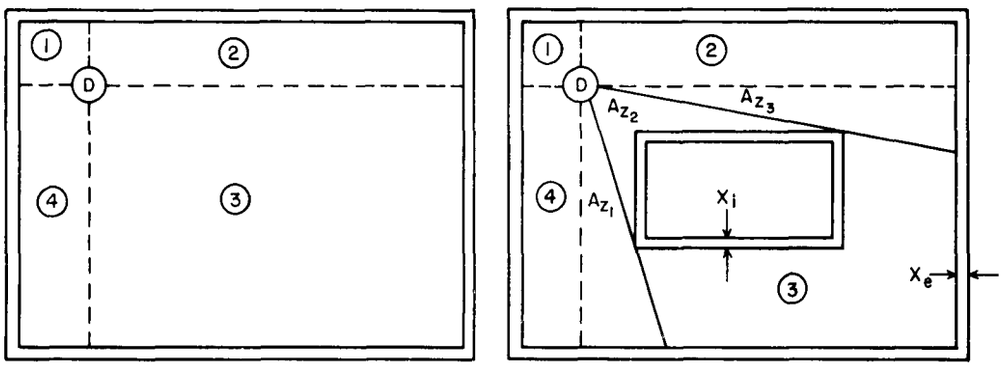

a. b.

Figure 9. Application of Geometric Terminology of Engineering Manual to Box Partition

The total dose rate arriving at a position in a corner of a structure with interior partitions may thus be written as

$$D_T = \frac{C_{g_1} + C_{g_2} + C_{g_4} + C_{g_3}\left[A_{z_1} + A_{z_3} + A_{z_2} B_w\left(2X_i, 3'\right)\right]}{4}$$

where

D_T = total dose rate

C_g = quadrant ground contribution without partitions

A_z = azimuthal angle of sector in degrees divided by 90^o

$B_w\left(2X_i, 3'\right)$ = barrier factor of interior partitions.

The off-center detector position in both the box geometry and corridor configurations was calculated by the general method described above. In the third geometry, that of compartmentation, perpendicular partitions were added to the corridor to subdivide the structure into rooms (see Figure 10a). The Engineering Manual method for taking these perpendicular partitions into account is illustrated in Figure 10b.

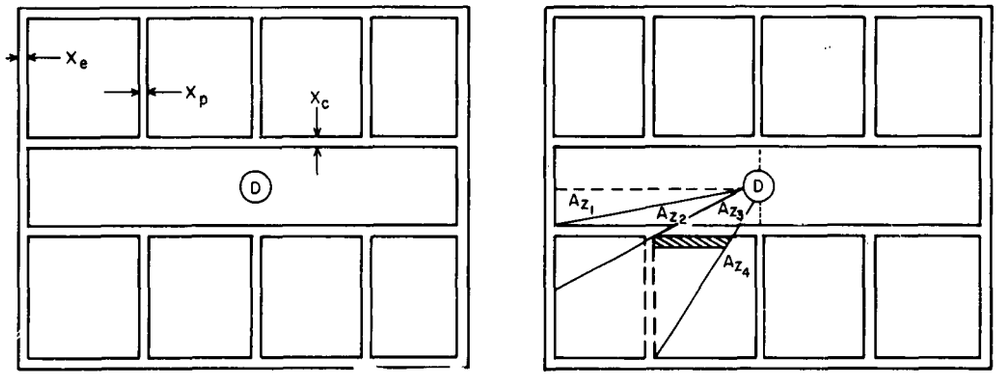

a. b.

Figure 10. Application of Geometric Terminology of Engineering Manual to Compartment Structure

Here again the ground contribution calculation is made by using the "position variation" and "azimuthal sector" procedures. In Figure 10b, four azimuthal sectors are shown, one of which is influenced by a perpendicular partition A_{z_3}. Azimuthal sectors A_{z_2} and A_{z_4} are influenced by the corridor wall, while azimuthal sector A_{z_1} is influenced by the exterior wall only. The procedure recommended in the Engineering Manual for handling multiple partitions is to add the mass thickness of each of these partitions, determine the appropriate barrier factor for their total thickness, and multiply the zero interior partition results by this factor. This is illustrated for the azimuthal sector A_{z_3}, which is influenced by the perpendicular partition, in Figure 10b. The calculation for the remainder of the quadrant is completed with the methods described above. This may be written as:

$$D_T^* = D_T \left[A_{z_1} + A_{z_2} B_w\left(X_i, 3'\right) + A_{z_3} B_w\left(X_i + X_p, 3'\right) + A_{z_4} B_w\left(X_i, 3'\right) \right]$$

where

D_T^* = total dose rate at the center position with partitions

D_T = dose rate at the center position without partitions

$B_w\left(X_i, 3'\right)$ = barrier factor for corridor wall

$B_w\left(X_i + X_p, 3'\right)$ = barrier factor for corridor wall plus perpendicular partition.

COMPARISON OF DATA

The purpose of the previous three sections has been to provide the analytical tools required to connect the data obtained from model experiments to those which would be obtained from similar full-scale experiments and to clearly outline the methods presently recommended in the Engineering Manual for the computation of the infinite-field dose rate in a compartmentalized structure. Thus, Eq. (1), evaluated in Table 6, presents the ratio of full-scale to model dose rate for any annulus of interest, and Eq. (3), evaluated in Table 7, presents the ratio of expected full-scale far-field dose to that obtained from the outer annulus of simulated contami-

nation used in the model experiments. Similarly, the previous section presents in outline form the computational methods presently proposed by the Engineering Manual to compute the dose rate within a compartmentalized structure.

BOX GEOMETRY

Experimental and calculated infinite-field ground dose rates are tabulated in Table 8 for the three interior partition mass thicknesses investigated. Dose rates for the basic building without interior partitions (0 psf partition mass thickness) are included for comparison. To facilitate such comparison, these results are presented graphically in Figure 11a for the center positions and in Figure 11b for the corner positions. Upon examination of Figures 11a and 11b it is obvious that the relative agreement between calculated and experimental values is excellent over all stories. Figure 11a shows that the absolute agreement between calculated and experimental

TABLE 8

COMPARISON OF MID-HEIGHT CALCULATED AND EXPERIMENTAL INFINITE-FIELD GROUND DOSE CONTRIBUTIONS, BOX PARTITIONS

Floor	Ground Dose Contribution (r/hr)*							
	Wall Thickness (psf)							
	Exterior 20 Interior 0		Exterior 20 Interior 20		Exterior 20 Interior 40		Exterior 20 Interior 60	
	Center Position Values							
	Experimental	Engr Manual	Experimental	Engr Manual	Experimental	Engr Manual	Experimental	Engr Manual
1	.36	.34	.24	.21	.15	.13	.096	.078
2	.24	.23	.16	.14	.098	.085	.064	.053
3	.18	.18	.12	.11	.074	.067	.049	.041
4	.15	.15	.099	.090	.061	.056	.041	.035
5	.12	.13	.081	.078	.049	.048	.033	.030
6	.10	.11	.068	.066	.042	.041	.029	.025
	Corner Position Values							
1	.41	.38	.38	.35	.36	.34	.37	.34
2	.28	.27	.28	.25	.27	.25	.27	.24
3	.22	.23	.22	.22	.21	.21	.21	.21
4	.20	.19	.19	.18	.18	.18	.18	.18
5	.17	.17	.17	.16	.16	.16	.17	.16
6	.15	.15	.15	.14	.14	.14	.15	.14

*Normalized to infinite-field strength that would give a 1 r/hr dose rate 3 feet above the field if the structure were absent.

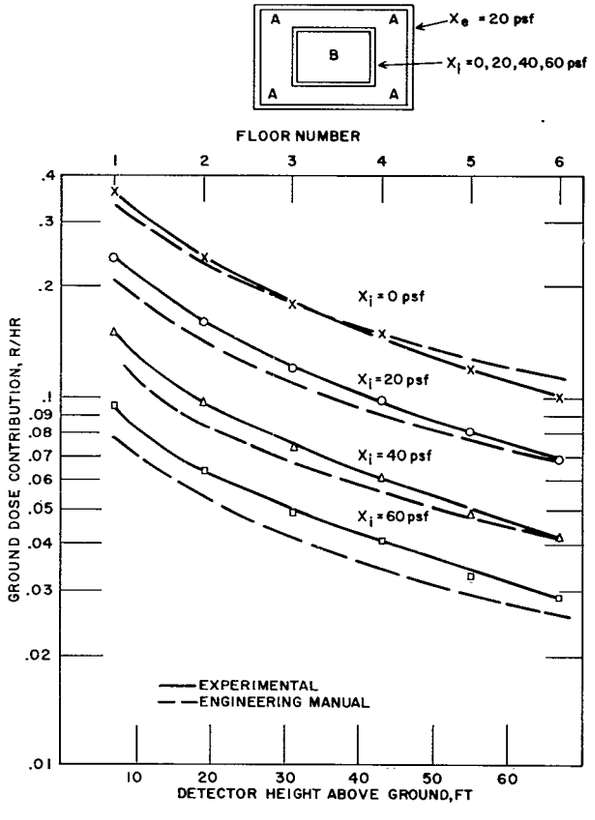

a. Detector Position B

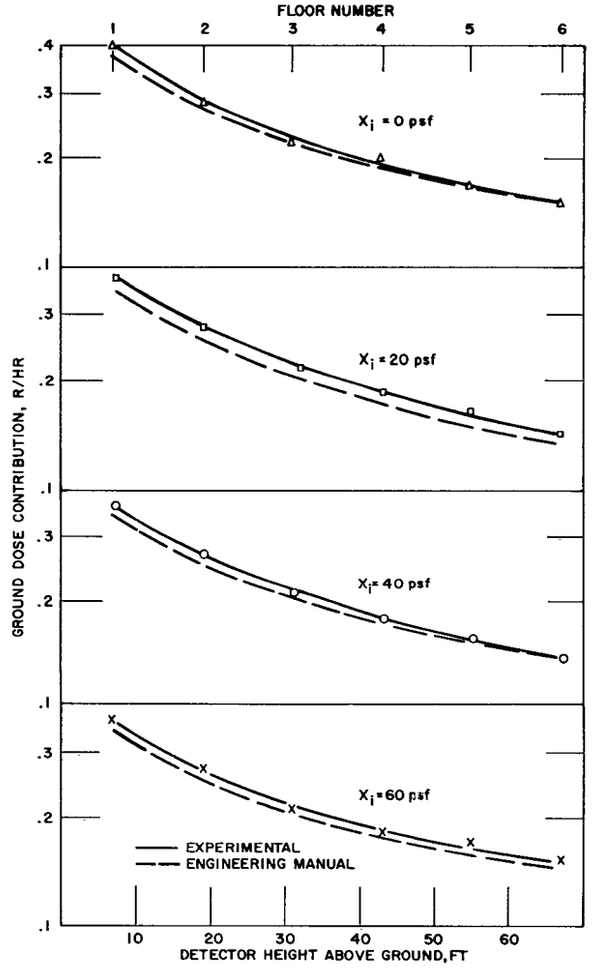

b. Detector Position A

Figure 11. Comparison of Calculated and Experimental Infinite-Field Dose Rates at Mid-Floor Detector Heights, Box Geometry (Normalized to field strength that gives 1 r/hr at 3 ft height)

values for the center positions is excellent for the 0 psf interior partition structure; however for the 20, 40, and 60 psf interior partition buildings, the Engineering Manual consistently underestimates the experimental results by 8, 10,and 15% respectively. Moreover, the absolute agreement of infinite-field ground contribution between the Engineering Manual and the experimental results for the corner positions (see Figure 11b) is excellent for all structures. From inspection of Table 8 it can be seen that increasing the mass thickness of the interior partitions from 20 to 60 psf had little or no effect on the corner positions.

CORRIDOR GEOMETRY

Experimental and calculated infinite-field ground dose rates are tabulated in Table 9 for the 20, 40, and 60 psf corridor walls. Values for the off-center positions within the corridor are also presented. These positions, known as D and F, were in the corridor 8 and 16 feet respectively from the center of the corridor. The results are presented graphically in Figure 12.

TABLE 9

COMPARISON OF MID-HEIGHT CALCULATED AND EXPERIMENTAL INFINITE-FIELD GROUND DOSE CONTRIBUTIONS, CORRIDOR PARTITIONS

Floor	Ground Dose Contribution (r/hr)*							
	Wall Thickness (psf)							
	Exterior 20 Corridor 0		Exterior 20 Corridor 20		Exterior 20 Corridor 40		Exterior 20 Corridor 60	
	Center Position Values							
	Experimental	Engr Manual	Experimental	Engr Manual	Experimental	Engr Manual	Experimental	Engr Manual
1	.36	.34	.23	.21	.15	.14	.10	.089
3	.18	.18	.11	.11	.074	.073	.050	.048
5	.12	.13	.075	.081	.049	.052	.032	.034
	Corner Position Values							
1	.41	.38	.35	.33	.33	.31	.32	.30
3	.22	.23	.20	.20	.19	.19	.18	.18
5	.17	.17	.16	.15	.15	.14	.15	.14
	D Position Values							
1	–	–	.23	.21	.16	.15	.11	.098
3	–	–	.12	.11	.081	.075	.054	.054
5	–	–	.082	.08	.051	.054	.036	.038
	F Position Values							
1	–	–	.27	.26	.20	.18	.14	.13
3	–	–	.14	.13	.10	.098	.074	.074
5	–	–	.099	.10	.074	.072	.055	.056

*Normalized to infinite-field strength that would give a 1 r/hr dose rate 3 feet above the field if the structure were absent.

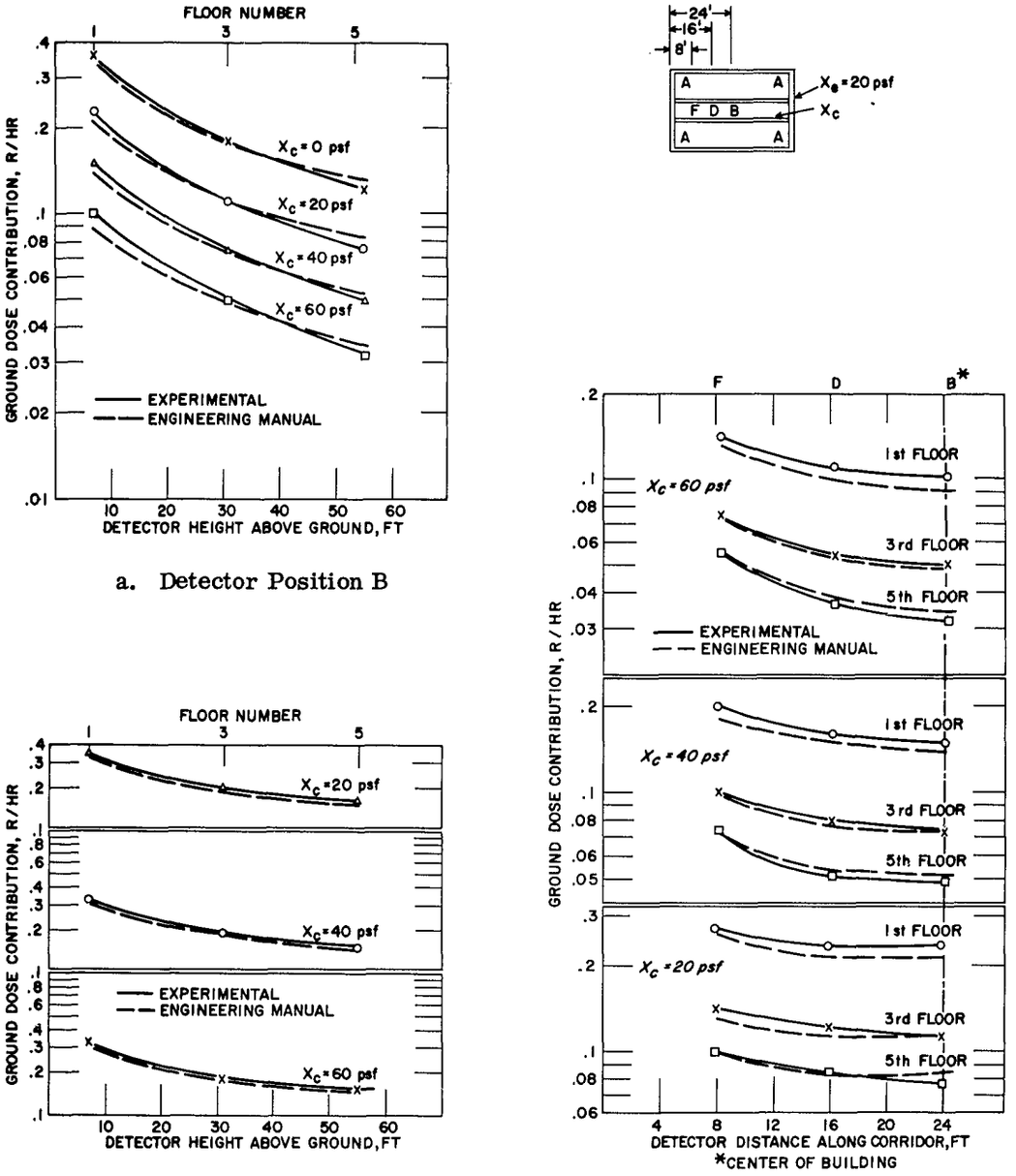

a. Detector Position B

b. Detector Position A

c. Detector Positions F, D, B

Figure 12. Comparison of Calculated and Experimental Infinite-Field Dose Rates at Mid-Floor Detector Heights, Corridor Geometry (Normalized to field strength that gives 1 r/hr at 3 ft height)

Agreement between calculated and experimental values for the center and corner positions is excellent over all stories (see Figures 12a and 12b); the agreement is within 7% for all corridor wall mass thicknesses investigated.

In Figure 12c dose rates versus distances along the corridor are plotted for the first, third, and fifth floors for 20, 40, and 60 psf corridor walls. Here again the agreement is excellent; the Engineering Manual underestimates the experimental dose rates on the first and third floors by about 8% and overestimates the dose rate in the fifth floor corridor by less than 5%.

COMPARTMENT GEOMETRY

Perpendicular interior partitions of 10, 20, and 40 psf were added to the corridor to form compartments for the third experiment. Measurements were made at 4-foot intervals in the corridor (see Figure 1c) to observe the effect of the perpendicular partitions on the dose rate within the corridor.

Experimental values are tabulated in Table 10 for all detector locations along with comparable calculated values for the center and corner locations and for two off-center corridor locations. As in the two previous configurations, there is excellent agreement between experimental and calculated values for both the center and corner positions. The dose rate versus detector height above the ground is plotted in Figure 13a for the center position and Figure 13b for the corner locations. It can be seen from Figure 13a that,unlike the two previous cases, the Engineering Manual overestimates the experimental dose rate at the center positions by about 8%, while underestimating the dose rate at the corner positions by less than 6% (Figure 13b).

To illustrate the effect of the perpendicular partitions upon the dose rate within the corridor and the variation with distance of the dose rate along the corridor, several plots are presented of dose rate versus detector location (Figure 13c) for the 10, 20, and 40 psf perpendicular partition configuration. The mass thickness of the corridor wall was 40 psf for this experiment.

Agreement between calculated and experimental values for detector locations inside the corridor is good. While agreement on the first floor is within 5%, discrepancies of the order of 10 to 15% occur on the third and fifth floors where the Engineering Manual predicts higher dose rates in all cases.

TABLE 10

COMPARISON OF MID-HEIGHT CALCULATED AND EXPERIMENTAL INFINITE-FIELD GROUND DOSE CONTRIBUTIONS, COMPARTMENT PARTITIONS (40 psf corridor wall)

Floor	Ground Dose Contribution (r/hr)*					
	Wall Thickness (psf)					
	Exterior 20 Compartment 10		Exterior 20 Compartment 20		Exterior 20 Compartment 40	
	Center Position Values					
	Experimental	Engr Manual	Experimental	Engr Manual	Experimental	Engr Manual
1	.13	.14	.12	.13	.10	.11
3	.065	.069	.060	.064	.051	.057
5	.041	.046	.040	.043	.035	.038
	Corner Position Values					
1	.31	.29	.30	.28	.29	.27
3	.18	.17	.18	.17	.17	.16
5	.15	.14	.14	.14	.14	.13
	C Position Values					
1	.12	–	.11	–	.090	–
3	.061	–	.055	–	.046	–
5	.041	–	.037	–	.032	–
	D Position Values					
1	.13	.13	.12	.12	.10	.10
3	.065	.073	.058	.064	.050	.056
5	.044	.053	.041	.044	.037	.042
	E Position Values					
1	.15	–	.14	–	.13	–
3	.081	–	.075	–	.066	–
5	.053	–	.052	–	.049	–
	F Position Values					
1	.17	.17	.16	.16	.15	.15
3	.092	.097	.087	.085	.078	.075
5	.066	.073	.066	.066	.062	.065
	G Position Values					
1	.23	–	.21	–	.21	–
3	.13	–	.13	–	.11	–
5	.094	–	.094	–	.093	–

*Normalized to infinite-field strength that would give a 1 r/hr dose rate 3 feet above the field if the structure were absent.

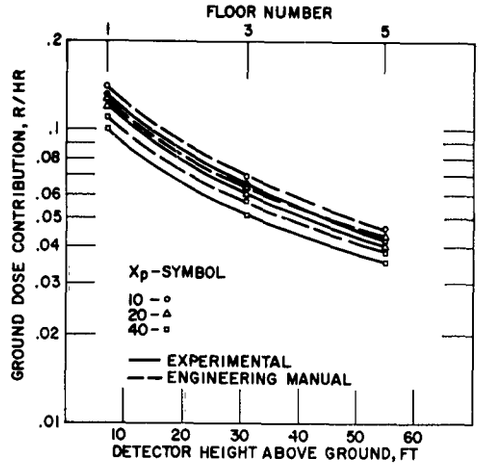

a. Detector Position B

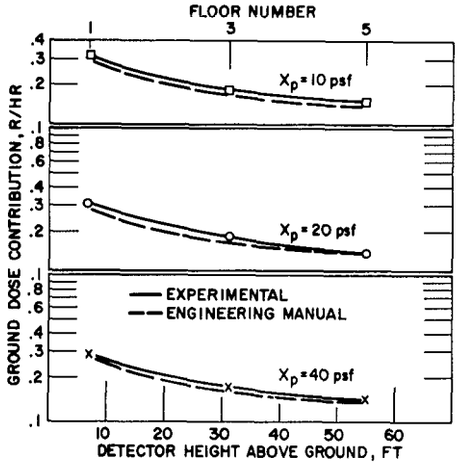

b. Detector Position A

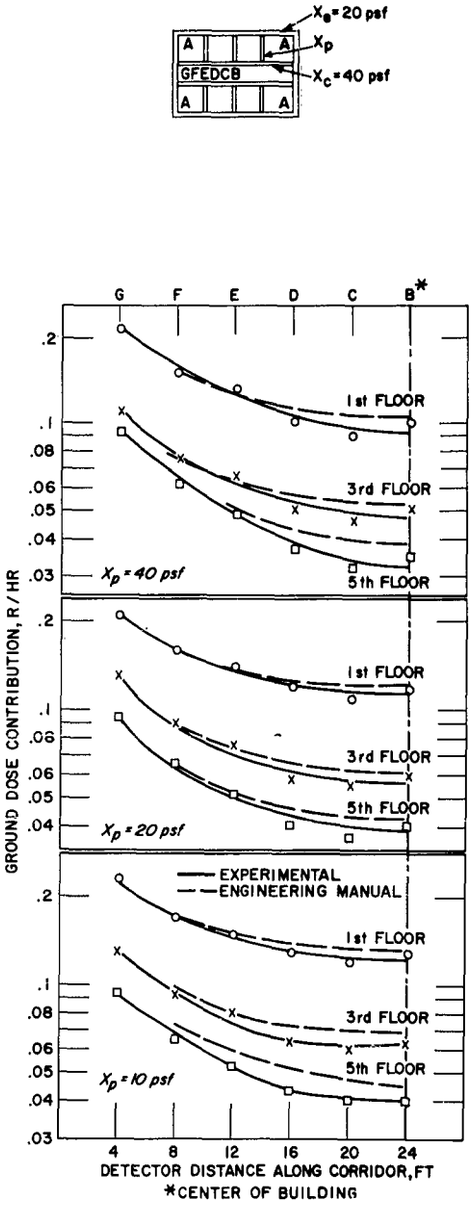

c. Detector Positions G, F, E, D, C, B

Figure 13. Comparison of Calculated and Experimental Infinite-Field Dose Rates at Mid-Floor Detector Heights, Compartment Geometry (Normalized to field strength that gives 1 r/hr at 3 ft height)

It should be noted here that in comparison with experimental dose rates inside the corridor with and without perpendicular partitions (see Figure 12c), the Engineering Manual overestimates the former and underestimates the latter.

LIMITED RECTANGULAR FIELDS OF CONTAMINATION

The contaminated fields simulated about the three geometric configurations of the model test structures were rectangular. It is thus of interest to compare the effects of limited fields of contamination about structures that had interior partitions of significant mass thickness with the effects obtained from similar structures that had no interior partitions (reported in Ref. 3). As demonstrated previously, a convenient method of presentation of the effects of limited rectangular strips of contamination is to plot the dose rate obtained from such a field, divided by the infinite-field dose rate for a similar detector position on the first floor versus field width W_c, divided by the detector height above ground. Table 11 presents the data previously obtained for structures of different floor and exterior wall thickness with no interior partitions for values of $W_c/h < 10$.

TABLE 11

FRACTION OF INFINITE-FIELD FIRST-FLOOR DOSE RATE*
(No Interior Partitions)

Width/Height (W_c/h)	Infinite-Field Dose Rate (r/hr)†					
	All Floors		First Floor		Upper Floors	
	0 psf Wall 20 psf Floor	20 psf Wall 20 psf Floor	20 psf Wall 80 psf Floor	80 psf Wall 80 psf Floor	20 psf Wall 80 psf Floor	80 psf Wall 80 psf Floor
0.0	0.0000	0.0000	0.0000	0.0000	0.0000	0.0000
0.32	0.0095	0.0057	–	–	0.00044	0.00047
0.44	0.017	0.0110	–	–	0.0011	0.0011
0.58	0.028	0.013	–	–	0.0024	0.0025
0.75	0.041	0.030	–	0.056	0.0044	0.0049
0.98	0.062	0.049	–	0.073	0.0083	0.010
1.33	0.089	0.078	–	0.095	0.015	0.019
2.06	0.14	0.14	–	0.14	0.033	0.045
2.5	0.17	0.17	0.11	0.17	0.044	0.063
5.0	0.30	0.31	0.25	0.30	0.15	0.17
10.0	0.46	0.48	0.42	0.48	0.33	0.32

*From Ref. 3, Tables 16, 17, 18, and 19 Mid-Height Center Position.

†Normalized to infinite-field strength that would give a 1 r/hr dose rate 3 feet above the field if the structure were absent.

The data obtained in this series of experiments for the center mid-height position of each floor are plotted as the cumulative total dose received from a rectangular contaminated field width W_c, divided by the infinite-field first-floor ground-contribution dose versus detector height h, divided by the field width W_c for the case of box partitions, corridor partitions, and compartment partitions (Figure 14, 15, and 16). The fraction of infinite-field dose rate obtained under similar conditions in a partitionless structure with 80 psf floors and 20 and 80 psf exterior walls are given in Table 11 for comparison.

It is clearly evident from an examination of Figures 14 through 16 that the fraction of infinite-field dose obtained from a limited rectangular field of contamination in a structure with interior partitions of significant thickness is nearly identical to that obtained in the absence of interior partitions. Thus data developed on the effects of limited fields of contamination in a structure without interior partitions may be safely used in computing such effects in a structure with partitions.

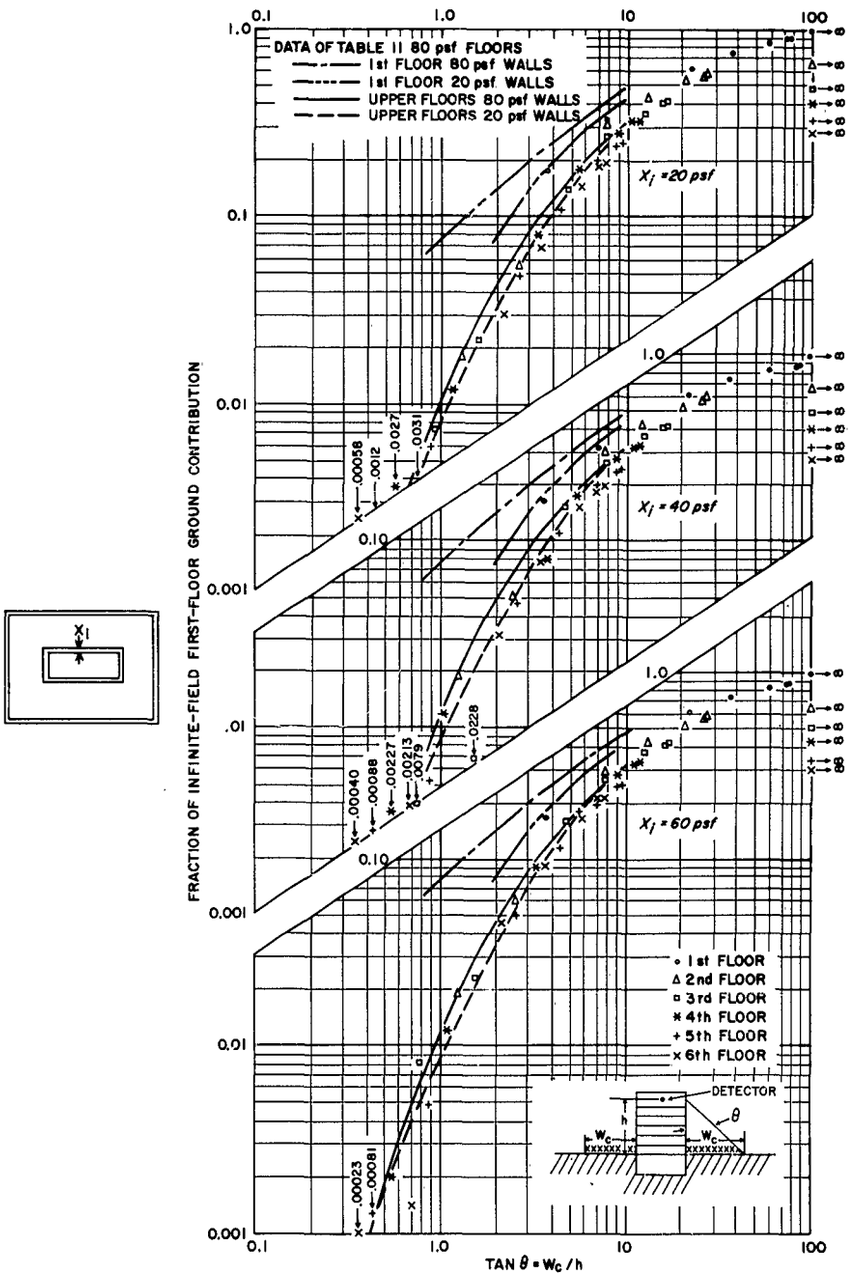

Figure 14. Fraction of Infinite-Field First-Floor Dose Rate for Mid-Height Center Position, Box Geometry

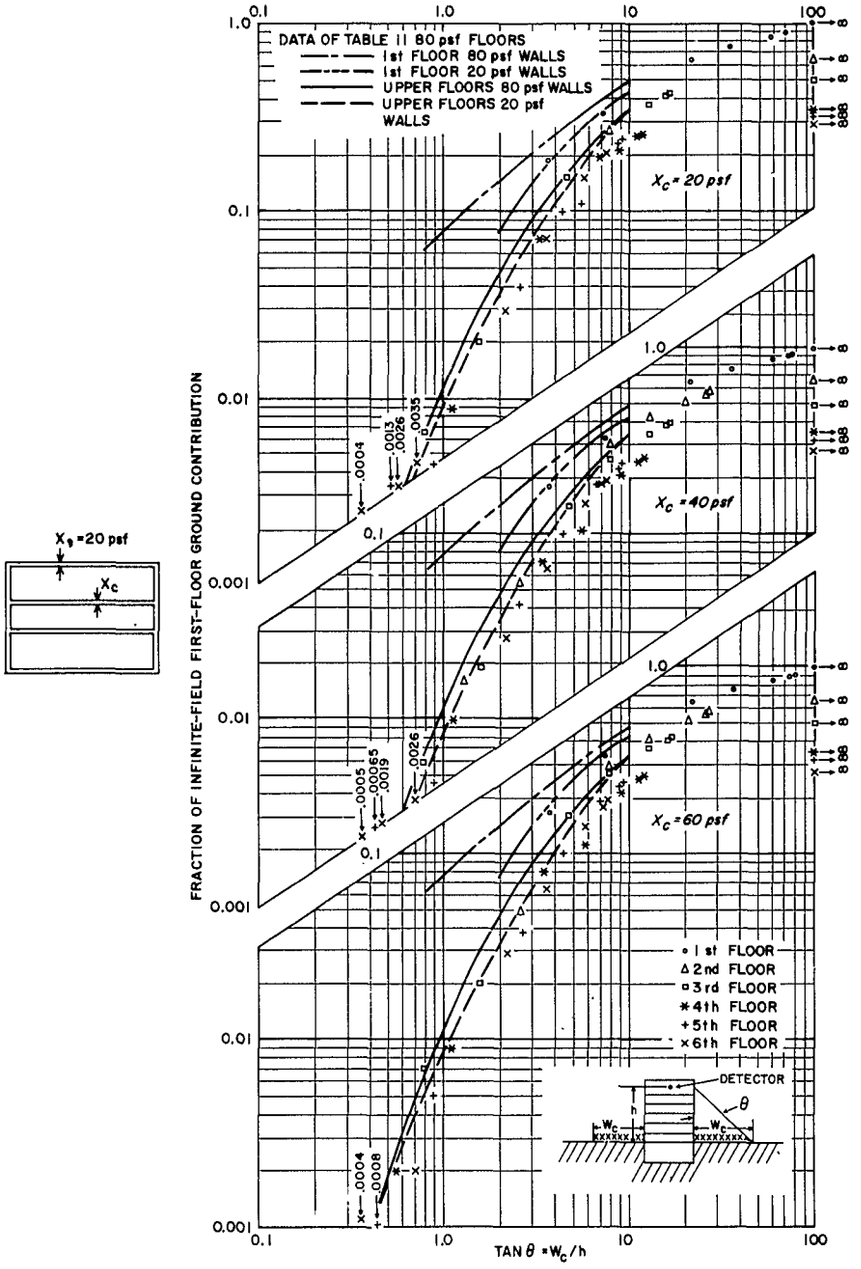

Figure 15. Fraction of Infinite-Field First-Floor Dose Rate for Mid-Height Center Position, Corridor Geometry

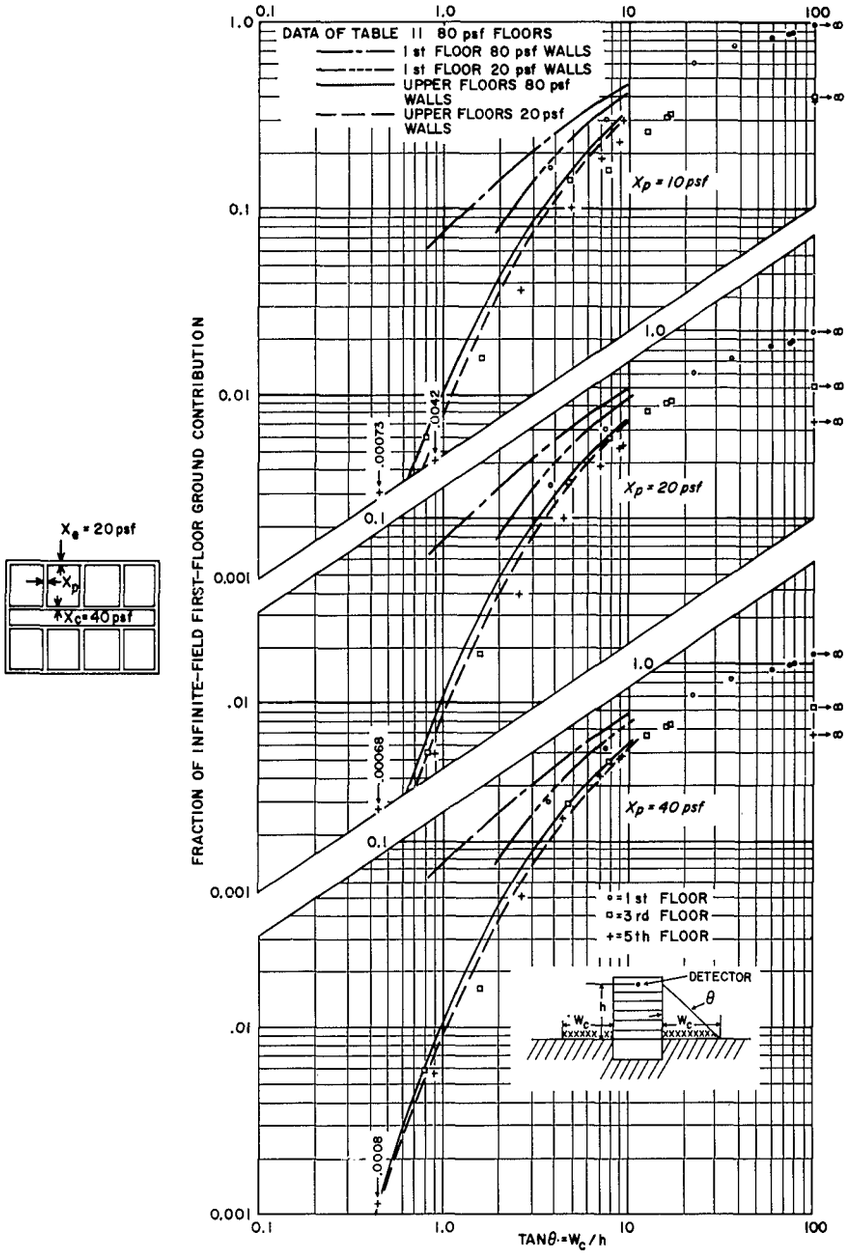

Figure 16. Fraction of Infinite-Field First-Floor Dose Rate for Mid-Height Center Position, Compartment Geometry

CHAPTER 4

CONCLUSIONS AND RECOMMENDATIONS

The purpose of this study has been to evaluate the procedures presented in the Engineering Manual for the computation of infinite-field radiation dose in a multi-story structure containing interior partitions of significant mass thicknesses and to investigate the effects of limited rectangular fields of contamination.

CONCLUSIONS

The major conclusions derived from this study may be summarized as follows:

1. The relative agreement between experimentally measured values of infinite-field dose rate and those computed using the methods of the Engineering Manual entitled "Design and Review of Structures for Protection from Fall-out Gamma Radiation" is excellent for the three configurations investigated.

   A. Box partitions. – The absolute agreement between calculated (Engineering Manual) and experimental values for the center position is excellent for the 0 psf interior partition structure, while for the 20, 40, and 60 psf interior partition buildings, the Engineering Manual consistently underestimates the experimental results by 8, 10, and 15% respectively. Agreement at the corner position is within 5%.

   B. Corridor partitions. – Agreement between calculated and experimental values for the center and corner positions is within 7% for all corridor wall mass thicknesses investigated. Agreement between calculated and experimental values for detectors located inside the corridor at the off-center positions is within 8% over all stories.

   C. Compartment partitions. – Agreement between calculated and experimental values for the center and corner positions is excellent. Calculated dose rates were between 10 and 15% higher than experimental dose rates for detector locations at the off-center positions inside the corridor.

2. For the interior partition geometries investigated in this study, a good estimate of the effects of interior partitions may be made by the following:

   A. Box and corridor geometries. — Multiply the dose rate computed in the center of the structure without interior partitions by the barrier attenuation factor (Ref. 1, Chart 1, Case 2) for a mass thickness equal to the interior wall thickness.

   B. Compartment geometries. — Multiply the dose rate computed in the center of the structure without interior partitions by the barrier factor for a mass thickness equal to the corridor walls plus one-half the compartment wall mass thickness.

3. Dose rates at corner positions for buildings with interior partitions of wall mass thicknesses less than 40 psf are about 10% less than those without partitions and 20% less for interior partitions of thicknesses greater than 40 psf.

4. The fraction of infinite-field dose obtained from limited rectangular fields of contamination in a structure with interior partitions of thickness several times greater than the exterior walls is identical to that obtained in a similar structure without interior partitions, times the barrier effect introduced by the partitions.

RECOMMENDATIONS

It is recommended that a survey of existing buildings be undertaken to determine if the mass thickness and interior partition configurations selected for this study are typical of those to be found in real structures.

If existing interior partition configurations are significantly different from those tested, further evaluation of the Engineering Manual is required.

REFERENCES

1. Office of Civil Defense, "The Design and Review of Structures for Protection from Fallout Gamma Radiation," rev. ed. (1 October 1961).

2. N. York, R. MacNeil, R. Brodeur, "The Effect of Limited Strips of Contamination on the Dose Rate in a Multistory Windowless Building, Volume IV, 20 psf Wall and 80 psf Floor Thickness," Technical Operations Research, Report No. TO-B 62-49 (July, 1962).

3. J. F. Batter, A. W. Starbird, and Nancy-Ruth York, "Final Report on the Effect of Limited Strips of Contamination on the Dose Rate in a Multistory Windowless Building," Technical Operations Research, Report No. TO-B 62-58 (August, 1962).

4. A. W. Starbird, J. F. Batter, and H. A. Mehlhorn, "Modeling Techniques as Applied to Fallout Simulation on Residential-Type Structures and Some Preliminary Results," Technical Operations Research, Report No. TO-B 61-35 (8 July 1961).

5. J. F. Batter and E. T. Clarke, "Modeling as a Technique for Determining Radiation Shielding," Shielding Symposium Proceedings, NRDL-OCDM Reviews and Lectures No. 110 (31 October - 1 November 1960).

6. J. F. Batter and A. W. Starbird, "The Effect of Limited Strips of Contamination on the Dose Rate in a Multistory Windowless Building, Volume I, 20 psf Wall and Floor Thickness," Technical Operations Research, Report No. TO-B 62-26 (30 April 1962).

7. J. F. Batter and A. W. Starbird, "The Effect of Limited Strips of Contamination on the Dose Rate in a Multistory Windowless Building, Volume II, 80 psf Wall and Floor Thickness," Technical Operations Research, Report No. TO-B 62-29 (15 May 1962).

8. J. F. Batter, A. W. Starbird, and M. Dwonczyk, "The Effect of Limited Strips of Contamination on the Dose Rate in a Multistory Windowless Building, Volume III, 0 psf Wall and 20 psf Floor Thickness," Technical Operations Research, Report No. TO-B 62-40 (30 June 1962).

9. E. T. Clarke, J. F. Batter, and A. L. Kaplan, "Measurement of Attenuation in Existing Structures of Radiation from Simulated Fallout," Technical Operations, Inc., Report No. TO-B 59-4 (27 April 1959).

10. E. T. Clarke and J. F. Batter, "Gamma-Ray Scattering by Nearby Surfaces," ANS Transactions 5 (1962).

11. L. R. Solon, and others, "Measurements of the Scatter Component from a Kilocurie Co-60 Source," U. S. AEC NYO-2065 (June, 1957).

12. R. E. Rexroad and M. A. Schmoke, "Scattered Radiation and Far-Field Dose Rates from Distributed Cobalt-60 and Cs-137 Sources," U. S. Army Chemical Corps, Nuclear Defense Laboratory, Report No. NDL-TR-2 (September, 1960).

13. B. L. Jones, J. W. Harris, and W. P. Kunkel, "Air and Ground Scattering of Co-60 Gamma Radiation," CVAC-170 (March, 1955).

14. L. V. Spencer, "Structure Shielding Against Fallout Radiation from Nuclear Weapons," National Bureau of Standards, Monograph 42 (1 June 1962).

Report No. TO-B 63-6
Starbird, A.W., Velletri, J.D., MacNeil, R.L., Batter, J.F., THE EFFECT OF INTERIOR PARTITIONS ON THE DOSE RATE IN A MULTISTORY, WINDOWLESS BUILDING. Technical Operations Research, Burlington, Mass. Office of Civil Defense, Department of Defense, Washington, D.C., 31 January 1963, 60 p. incl. 16 figs., 11 tables.

Unclassified Report

This report evaluates the effects of three common types of interior partitions within multistory structures on the dose rates from infinite uniform fields of fallout contamination. Comparisons are made between experimentally determined steel model results utilizing cobalt-60 gamma radiation and those obtained through use of the OCD engineering manual entitled "Design and Review of Structures from Fallout Gamma Radiation." A comparison is also made between partition results from limited fields of contamination and previous experimentally determined limited-field results for similar structures without partitions.

Agreement is excellent between experimentally measured and computed infinite-field dose rates for the three partition geometries compared — typical box, corridor, and compartment types.

(over)

1. The Effect of Interior Partitions on the Dose Rate in a Multistory, Windowless Building
2. Simulated Fallout
3. Co-60
4. Modeling Technique
5. Radiation Shielding
6. Starbird, A.W.
7. Velletri, J.D.
8. MacNeil, R.L.
9. Batter, J.F.
10. Office of Civil Defense
11. Contract OCD-OS-62-14

Report No. TO-B 63-6
Starbird, A.W., Velletri, J.D., MacNeil, R.L., Batter, J.F., THE EFFECT OF INTERIOR PARTITIONS ON THE DOSE RATE IN A MULTISTORY, WINDOWLESS BUILDING. Technical Operations Research, Burlington, Mass. Office of Civil Defense, Department of Defense, Washington, D.C., 31 January 1963, 60 p. incl. 16 figs., 11 tables.

Unclassified Report

This report evaluates the effects of three common types of interior partitions within multistory structures on the dose rates from infinite uniform fields of fallout contamination. Comparisons are made between experimentally determined steel model results utilizing cobalt-60 gamma radiation and those obtained through use of the OCD engineering manual entitled "Design and Review of Structures from Fallout Gamma Radiation." A comparison is also made between partition results from limited fields of contamination and previous experimentally determined limited-field results for similar structures without partitions.

Agreement is excellent between experimentally measured and computed infinite-field dose rates for the three partition geometries compared — typical box, corridor, and compartment types.

(over)

1. The Effect of Interior Partitions on the Dose Rate in a Multistory, Windowless Building
2. Simulated Fallout
3. Co-60
4. Modeling Technique
5. Radiation Shielding
6. Starbird, A.W.
7. Velletri, J.D.
8. MacNeil, R.L.
9. Batter, J.F.
10. Office of Civil Defense
11. Contract OCD-OS-62-14